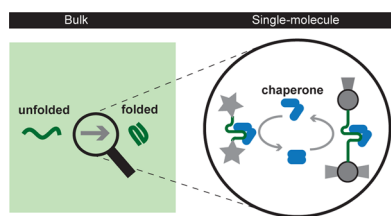


## Chaperone Action at the Single-Molecule Level

Alireza Mashaghi,<sup>\*,†</sup> Günter Kramer,<sup>‡</sup> Don C. Lamb,<sup>§</sup> Matthias P. Mayer,<sup>‡</sup> and Sander J. Tans<sup>\*,†</sup><sup>†</sup>AMOLF Institute, Science Park 104, 1098 XG Amsterdam, The Netherlands<sup>‡</sup>Zentrum für Molekulare Biologie der Universität Heidelberg (ZMBH), DKFZ-ZMBH Allianz, Im Neuenheimer Feld 282, 69120 Heidelberg, Germany<sup>§</sup>Physical Chemistry, Department of Chemistry, Munich Center for Integrated Protein Science (CiPSM) and Center for Nanoscience, Ludwig-Maximilians-Universität München, Butenandtstrasse 5-13, Gerhard-Ertl-Building, 81377 Munich, Germany

## CONTENTS

1. Introduction	660
1.1. Structure and Dynamics of Three Chaperones: Knowns and Unknowns	661
1.1.1. HSP60	661
1.1.2. HSP70	663
1.1.3. HSP90	663
2. Single Molecule versus Bulk Studies	663
3. Single-Molecule Experiments on Chaperones and Assisted Protein Folding	665
3.1. Single-Molecule Techniques—Fluorescence Methods	666
3.1.1. Single-Pair Förster Resonance Energy Transfer (FRET)	666
3.1.2. Fluorescence Correlation Spectroscopy (FCS)	666
3.1.3. Photoinduced Electron Transfer (PET)	666
3.2. Single Molecule Techniques—Force Methods	666
3.2.1. Atomic Force Microscopes (AFM)	666
3.2.2. Optical Tweezers	666
3.2.3. Solid-State Nanopores	666
3.3. Initial Single-Molecule Experiments on Chaperones and Folding	667
3.4. Fluorescence Experiments	667
3.5. Force Spectroscopy and Pulling Experiments	669
3.6. In Silico Single-Molecule Methods	670
4. Conclusion	671
Author Information	673
Corresponding Authors	673
Author Contributions	673
Funding	673
Notes	673
Biographies	673
Acknowledgments	674
References	674

## 1. INTRODUCTION

Natively folded proteins generally have a significant number of hydrophobic residues that cluster together to form a hydrophobic core. However, during the vectorial synthesis on the ribosome and subsequent folding, these hydrophobic residues are exposed. Because folding occurs in a highly crowded environment, exposed residues can lead to undesired interactions that irreversibly harm the folding process. In particular, they can result in the formation of misfolded states and aggregation.<sup>1</sup> There are ample opportunities for such undesired interactions to occur during folding. While secondary structures form on the order of microseconds or faster, folding into the tertiary structure may take up to minutes.<sup>2</sup> In the meanwhile, proteins are diffusing through the highly crowded cellular environment on subsecond time scale.<sup>3,4</sup> Newly synthesized polypeptides hence can interact with a multitude of cellular components before they gain their native fold. Once properly folded, proteins are at a reduced risk of pathological interactions. However, even when folded, thermodynamic fluctuations in protein structure, especially at elevated temperatures, can induce partial unfolding and misfolding, which in turn increases the probability of unwanted intermolecular interactions.<sup>5</sup>

To mitigate the risk of erroneous interactions, cells are equipped with numerous types of molecular chaperones (see Table 1, Figure 1) that employ a wide array of molecular mechanisms (see section 1.1). Briefly, chaperones may be involved in tasks such as assisting in *de novo* folding, assembly of protein complexes, and membrane insertion and translocation, as well as protein refolding. ATP-independent chaperones such as trigger factor, SecB, and the small heat shock proteins (HSPs) are believed to act as “holdases” that suppress the aggregation of exposed polypeptide chains and delay folding. Chaperonins (HSP60) and HSP70 are more complex chaperone systems of multiple components that can promote folding through cycles of ATP-driven binding and release of their client proteins. Chaperones of different families may act on the same protein, assisting different folding steps. For instance, ribosome-associated chaperones (trigger factor in prokaryotes and plastids, Hsp70s and NAC in eukaryotes) already act cotranslationally. For many polypeptides, this interaction is believed to be sufficient for folding. Proteins with more complex folding trajectories may then bind to downstream acting chaperone systems including Hsp70s and

Received: March 5, 2013

Published: September 3, 2013

Table 1. Chaperone Families, Classes, and Their Functions

cellular chaperone family	prokaryote	eukaryote	function
Hsp70	DnaK	Hsc73 (cytosol), BiP (ER), SSC1 (mitochondria), ctHSP70 (chloroplast)	promotes de novo folding of polypeptides and refolding of denatured proteins; acts as unfoldase(?)
Hsp90	HtpG	Hsp90 (cytosol), Grp94 (ER)	chaperones late folding intermediates
ribosome-associated chaperones	trigger factor	trigger factor (chloroplast) RAC, Ssb, NAC (yeast) Mpp11, and Hsp70L1 (higher eukaryotes)	folding assistance for newly synthesized proteins, peptidyl-prolyl cis–trans isomerase (PPIase) activity; the function of NAC in protein folding is not established and it lacks PPIase activity
chaperonin/Hsp60	GroEL/GroES	CCT/TRiC (cytosol), Hsp60 (mitochondria), Cpn60 (chloroplast)	promotes de novo folding of polypeptides and refolding of denatured proteins
Hsp100	ClpB, ClpX, ClpA/C	Hsp104, Hsp78 (mitochondria)	protein disaggregation and unfolding; some are in complex with a proteinase subunit
small Hsps	IbpA, IbpB	numerous members	prevention of aggregation, assistance in disaggregation
SecB	SecB		stabilization of translocation intermediates

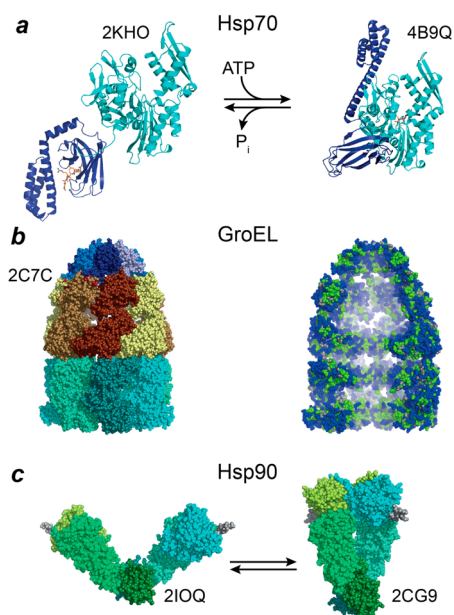


**Figure 1.** Structures of representative molecular chaperones. (a) Hsp70 chaperones, left structure, cartoon representation of the structure of the *Escherichia coli* Hsp70 homologue DnaK in the absence of nucleotides or in the presence of ADP (PDB code 2KHO<sup>6</sup>); right structure, cartoon representation of *E. coli* DnaK in the ATP-bound open conformation (PDB code 4B9Q<sup>7</sup>). Nucleotide binding domain is colored cyan and substrate binding domain dark blue. (b) Hsp60 chaperones, left structure, space-filling representation of *E. coli* GroEL in complex with GroES and bound ATP (PDB code 2C7C<sup>8</sup>). The GroES subunits are shown in shades of blue, GroEL subunits of cis-ring in yellow and brown, and GroEL subunits of trans-ring in cyan and green. right structure, same structure as the left structure with three of the seven subunits removed and colored according to hydrophobicity, with hydrophobic residues in green (Met, Leu, Ile, Val, Ala, Phe, Tyr, Trp) and hydrophilic residues in blue (Lys, Arg, Glu, Asp, Asn, Gln, Ser, Thr, His). (c) Open and closed conformation of Hsp90 dimer. Left structure, space-filling representation of nucleotide-free *E. coli* HtpG (PDB code 2IQ9<sup>9</sup>). Right structure, space-filling representation of yeast Hsp82 in complex with AMPNP and the cochaperone Sba1 (latter not shown) (PDB code 2CG9<sup>10</sup>). Hsp90 is colored according to the domain structure with the nucleotide binding domain shown in light green and cyan, middle domain in green and turquoise, and the dimerization domain in dark green and dark teal.

chaperonins or be transferred onto Hsp90s.<sup>11</sup> Chaperones also cooperate with each other. Under stress conditions, misfolded proteins frequently coaggregate with sHSP, which facilitates

subsequent disaggregation and refolding by concerted action of Hsp70 and Hsp110 in metazoans or Hsp70 and Hsp100 in other organisms.<sup>12</sup> Hsp70 and Hsp90 also cooperate with each other in the control of stability and activity of many native regulatory proteins.<sup>13</sup>

Considerable knowledge has been amassed over the past decades on the molecular mechanisms of chaperones, yet many fundamental questions remain unanswered. Specifically, we know little about how chaperones influence the conformation of client proteins during folding, which is considered to be central to chaperone function. Chaperones are thought to act both as suppressors of aggregation and as folding catalysts, but distinguishing both roles remains a challenge. The physical principles that chaperones exploit are also often unclear. Chaperones may affect the entropy of unfolded chains, lower reaction barriers by stabilizing intermediates, or guide the conformation of the protein chain (e.g., by preventing off-pathway intermediates). Questions also remain on the precise role of energy input, the dynamics of chaperone conformational changes, its relation to protein client dynamics, and how chaperones can act in a generic manner on many different proteins.

These questions are difficult to address with bulk techniques because the underlying molecular mechanisms involve interactions that are often transient and heterogeneous. Single-molecule approaches have allowed the study of isolated proteins in real time, thereby revealing the rich conformational dynamics of proteins during the folding process. This capability makes single-molecule methods ideally suited to address many of the open questions with respect to chaperone function. In recent years, a start has been made to study chaperone-assisted protein folding using single-molecule techniques. Many excellent reviews on unassisted protein folding and on bulk studies of chaperones have been published.<sup>14</sup> However, the emerging single-molecule studies of chaperones and assisted protein folding have so far received little attention. Here, we review a number of studies that address the folding of proteins aided by chaperones at the single molecule level. This will be preceded by an overview of the main chaperone systems and a discussion of the nature of single molecule assays as compared to bulk measurement techniques. We highlight how single-molecule methods can be used to answer the key questions related to assisted-protein folding reactions.

## 1.1. Structure and Dynamics of Three Chaperones: Knowns and Unknowns

### 1.1.1. HSP60.

These chaperones, called chaperonins, are thoroidal double-ring complexes of ~800–900 kDa with a

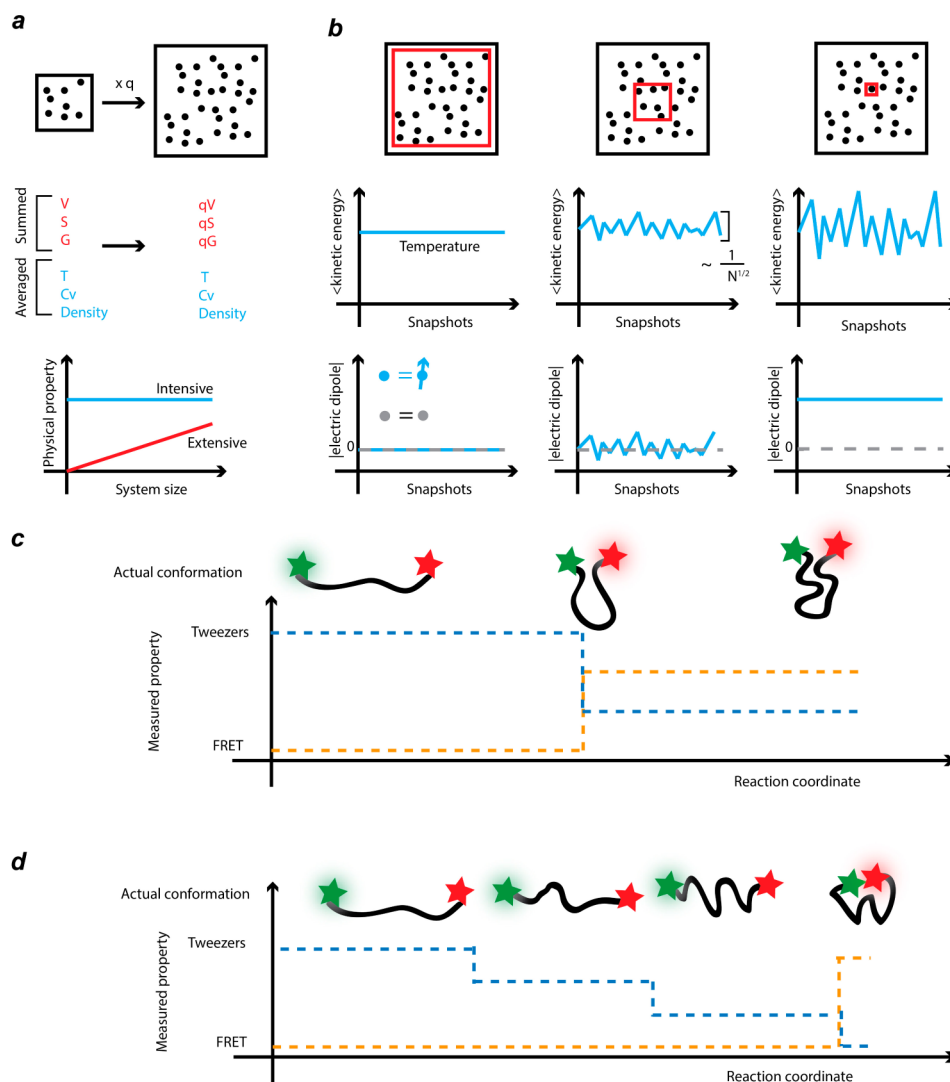


**Figure 2.** Advantages and limitations of single molecule techniques. (a) In thermodynamics, extensive and intensive properties of a large system are the result of sum and averaging performed on individual molecular properties. For a system composed of gas molecules, extensive properties such as free energy ( $G$ ), entropy ( $S$ ), and volume ( $V$ ) scale with the size of the system. Intensive properties such as temperature ( $T$ ) do not scale with the system size and remain invariant upon scaling. (b) Illustration of the key differences when an intensive property is measured at bulk and single-molecule scales. Average kinetic energy measurement at large scale provides a signal with negligible noise. The noise varies inversely with the square root of the number of molecule under study. The noise however might carry useful information. Electric dipole moment (per molecule) measurements in bulk for example cannot distinguish between a solution of polar molecules and a solution of nonpolar molecules, as the dipoles will cancel out due to random orientation of molecules. When measurements are performed on a mesoscopic sample, the electric dipole of the polar molecule appears as the measurement noise. Single-molecule measurement provides the magnitude of the dipole moment precisely. (c, d) An example conformation of a protein along a folding trajectory. In single-molecule experiments, the state of a molecule with many degrees of freedom is identified by one or a few detected properties, for example, a FRET signal or the end-to-end distance measured by optical tweezers. (c) Trajectory with a single folding transition. In this case, a long-range interaction is formed early in the folding process. The end-to-end distance and FRET signal are both degenerate properties after the transition. (d) For proteins that fold via different distinct states that grow in size, some folded states may not be distinguished in the FRET signal, as it is sensitive in particular in the range of 1–10 nm;<sup>40</sup> optical tweezers have a wider length range but require an applied force that can perturb the folded state.

central folding chamber in each ring<sup>15</sup> (Figure 1b). They are divided into two classes. Class I or GroEL-type chaperonins, existing in prokaryotes, mitochondria and chloroplasts, consist of seven identical subunits per ring and cooperate with the 7-mer cochaperone GroES, which functions as lid for the folding chamber. Class II chaperonins, existing in eukaryotes and archaeons (TCP or TRiC), consist of eight or nine identical or different subunits per ring and contain a built-in lid. The best understood Hsp60 is the GroEL/GroES system of *E. coli*. Proteins up to ~60 kDa are enclosed in the central chamber underneath the GroES lid. GroEL/GroES can also fold larger

proteins by a “trans” mechanism without enclosure in the cavity.<sup>16</sup> Clients that are dependent on GroEL/GroES for folding typically have  $\alpha/\beta$  or  $\alpha+\beta$  domain topologies.<sup>17</sup> Each chaperonin subunit consists of three domains: an equatorial domain, which binds ATP and forms inter-ring contacts; an intermediate domain; and an apical domain, which interacts with substrates and GroES in the case of GroEL. The apical domains present hydrophobic amino acid residues in the ring center for substrate binding. GroEL/GroES cycles through a number of allosteric states including the nucleotide-free T state, with high affinity for substrate proteins, and the ATP-bound R

state.<sup>18</sup> Binding of ATP and GroES to the substrate bound “cis” ring induces a conformational change that rotates the intermediate and apical domains such that the hydrophobic substrate binding patches are hidden and substrate is released into the hydrophilic closed cavity.<sup>15a,19</sup> GroES is dissociated at a time scale of  $\sim 15$  s, triggered by ATP binding to the opposite “trans” ring.<sup>14a</sup> Steric confinement of substrate within the GroEL/ES cavity can assist protein folding directly<sup>20</sup> or indirectly by suppressing aggregation.<sup>21</sup> Open questions remain about the pathways by which allosteric states of GroEL interconvert and how GroEL/ES activity affects folding pathways of client proteins. This is because of the transient nature of the intermediates, the potential multiplicity of pathways, and the difficulties in measuring networks of energetic connectivity in large systems.<sup>22</sup>

**1.1.2. HSP70.** A family of highly conserved chaperones that is present in all domains of life and in most subcellular compartments. Hsp70 consists of an N-terminal nucleotide binding domain and a C-terminal domain (Figure 1a) that can bind exposed polypeptide chains co- and post-translationally in a binding groove and clamp them with a moveable lid.<sup>23,6,24</sup> In the nucleotide-free and ADP-bound state, substrate affinity is high, while binding and release rates are low. ATP increases peptide association and dissociation rates by several orders of magnitude and decreases the affinity for substrates by 10–50-fold.<sup>25</sup> These data indicate that the C-terminal domain of Hsp70s assumes different conformational states depending on the nucleotide status of the nucleotide binding domain, including a closed and open conformation. For some of these conformations, structural data exist.<sup>7,26</sup> ADP-bound HSP70 populates a closed, an open and a widely open state, with the former being the prominent species.<sup>27,28</sup> Key to Hsp70 function is the association of Hsp70-ATP to clients with high rates and subsequent trapping by ATP hydrolysis for tight binding. However, intrinsic ATPase rates of Hsp70 are very low (1 ATP per 20–30 min). This ATPase rate is stimulated by the protein client itself and by a cochaperone of the J-domain protein family. Subsequent client release is triggered by nucleotide exchange factors, which accelerate dissociation of ADP, allowing rebinding of ATP and conversion into the open ATP bound low affinity state. HSP70s can improve refolding rates of denatured proteins *in vitro*,<sup>29,30</sup> and rescue misfolded<sup>31</sup> and aggregated proteins.<sup>12a,c,32</sup>

One of the characteristics of Hsp70s is that they appear to promiscuously bind practically all proteins in a nascent, misfolded, or aggregated state but do not interact with their folded counterpart. This promiscuous binding is consistent with its rather generic recognition motif, which consists of a core of up to five hydrophobic residues flanked by positively charged residues.<sup>33</sup> Such motifs are found on average every 30–40 residues in most protein sequences. They mostly reside in the hydrophobic core of folded proteins and are only exposed during synthesis or upon denaturation. How Hsp70 refolds denatured proteins is a matter of debate. There are indications that Hsp70s can promote local unfolding of misfolded or even certain native proteins.<sup>31,34</sup> Hsp70 also promotes degradation of proteins that cannot be refolded. This protein triage decision seems to have a stochastic component: proteins that spend more time being bound to Hsp70 have a higher chance of being ubiquitinated.<sup>35</sup> Many questions remain regarding the client–HSP70 interaction. Are Hsp70s able to induce unfolding or do they select unfolded states out of an ensemble of conformational states of the client protein? Is folding indeed promoted

by clamping and releasing exposed polypeptides and, if so, how?<sup>36</sup> Is the energy of ATP hydrolysis merely used to drive the cycle forward or is it directly used for folding?

**1.1.3. HSP90.** The 90 kDa heat shock family of proteins exist in all kingdoms of life. Hsp90s are ATP-driven homodimeric chaperones (Figure 1c) that interact with a wide range of client proteins, which are bound in a native or near-native conformation. Hsp90s are built-up of three domains: an N-terminal nucleotide binding domain, a middle domain involved in ATP hydrolysis, and a C-terminal dimerization domain.<sup>9,10</sup> All three domains have been implicated in substrate binding. The ATP-driven reaction cycle is accompanied by substantial structural rearrangement.<sup>14d</sup> In the nucleotide-free or ADP-bound state, Hsp90 is in equilibrium between the wide-open and closed V-shaped conformations. ATP binding leads to dimerization of the N-terminal domains, resulting in a compaction of the dimer in which the monomers twist around each other. After ATP hydrolysis, the nucleotide binding domains dissociate, and the HSP90 protomers separate N-terminally. Separation of the C-terminal dimerization domains has also been observed and seems to be anticorrelated with the N-terminal domains.<sup>37</sup> Hsp90 cooperates with the Hsp70 system and its chaperone cycle is regulated in eukaryotic cells by a large number of cochaperones, which influence the ATPase rate, act as scaffolding proteins, and target clients to Hsp90. Open questions include the following: Where do clients bind, or are there several sites?<sup>38</sup> How does Hsp90 movement and the diverse cochaperones affect client folding? How is Hsp90 function affected by post-translational modifications?

## 2. SINGLE MOLECULE VERSUS BULK STUDIES

Conventional biochemical assays involve millions of billions of molecules often reacting within an aqueous environment. The measured molecular properties are then summed or averaged over an ensemble of molecules as described in statistical thermodynamics (Figure 2a). This leads to a high signal-to-noise ratio but also to information loss (Figure 2b). To illustrate this point, consider the following example. Proteins in solution carry kinetic energy and often have significant electric dipole moments that affect their interactions. Measurement of the kinetic energy—i.e., the temperature of the protein solution—can be done precisely in bulk, while fluctuations become apparent and, as a consequence, the signal-to-noise ratio reduces when the measurements are performed on a small subsystem (Figure 2b). However, the fluctuations themselves carry information that may be of interest. When the net dipole moment of the system is measured in bulk, the dipoles will sum to zero for a solution of proteins with negligible intermolecular coupling. In this case, measurement of the total dipole moment on a smaller scale will help the observer to distinguish between a protein solution and a solution containing nonpolar molecules. In exceptional cases, the loss of information due to ensemble averaging and lack of synchrony can be partly circumvented in ensemble measurements. For example, when molecules are embedded in anisotropic environments, their residual internuclear magnetic dipolar coupling (which is averaged to zero in solution NMR studies) will be detectable in bulk due to partial alignment of molecules. The use of this approach to recover structural information from dipolar coupling has provided new insights into the folding of the spliceosome, an RNA–protein complex responsible for mRNA splicing in cells.<sup>39</sup>

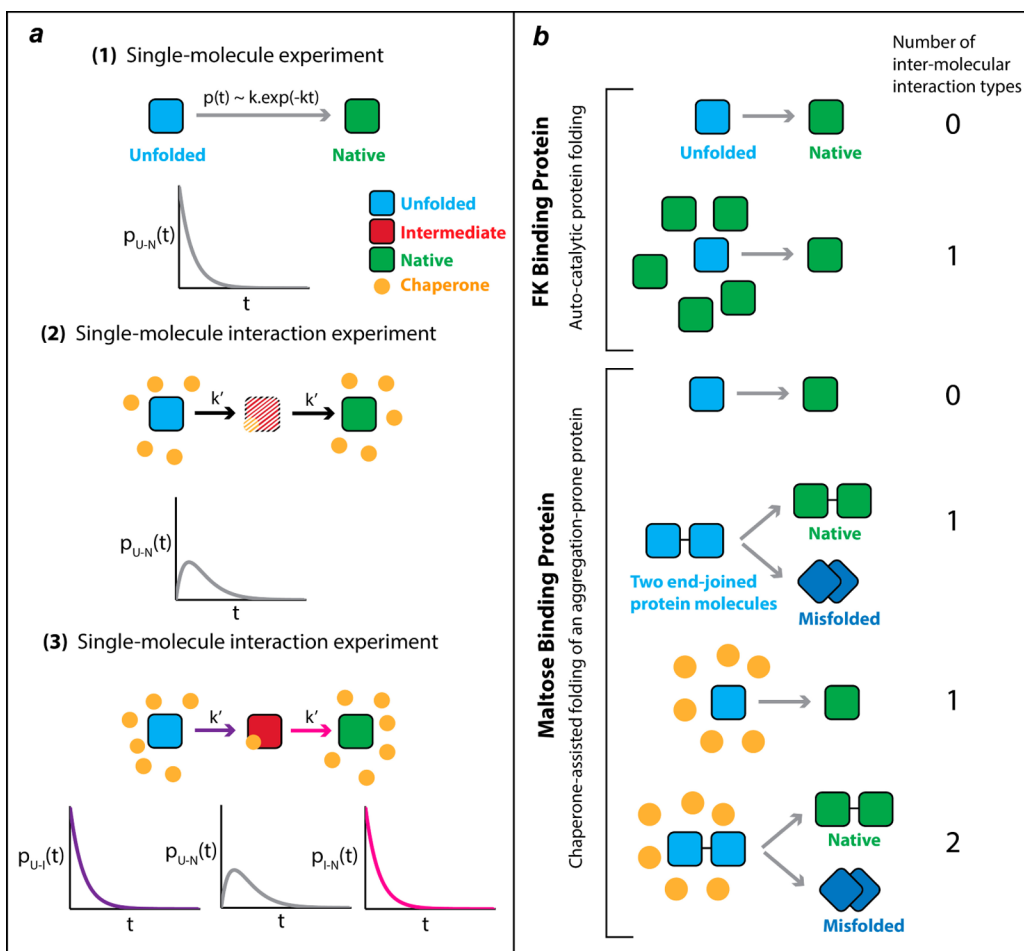


**Figure 3.** Benefits of single-molecule approaches for probing chaperone-mediated protein folding. (a) Single-molecule techniques allow for indirect and direct detection of chaperone induced folding intermediates. Three scenarios are presented. In scenario 1, single step (two-state) protein folding, the state of the protein is monitored in time as the protein transits from unfolded state to folded state. The constructed distribution of measured dwell times follows a single exponential decay. When chaperones are present, they may change the folding rate without changing the number of conformational states visited during folding. In this case, the constructed distribution of dwell times follows a single exponential decay with a different rate constant. Alternatively, the folding pathway of a two-state folder might change in the presence of chaperones by emergence of intermediate states, as indicated in scenarios 2 and 3. The emergence of intermediates renders the probability distribution of the dwell time nonexponential. In scenario 2, the intermediate molecule is not directly observed (striped red square). However, from the shape of the probability distribution, it might be possible to decipher the number of intermediate steps. In scenario 3, all molecular species are directly detectable and reaction rates can be measured directly. (b) Single-molecule techniques allow for controlling the number of possible intermolecular interactions and taking a reductionist approach. Intermolecular interactions may lead to nonlinearity of the kinetics and emergence of competing reaction pathways. Two examples are illustrated: FKBP prolyl isomerase, a protein that self-interacts and catalyzes its own folding, and MBP, a protein that self-interacts and forms an aggregate. The schematics show how with different experimental designs one can allow some selected interactions to happen while preventing others.

Within the last 20 years, it has become possible not only to detect individual molecules but also to perform measurements on single molecules. In principle, performing measurements over a prolonged period of time on a single molecule would provide the same information as bulk measurements when the system is ergodic. Ergodicity is common in molecular systems (with some exceptions like systems with symmetry breaking<sup>41</sup>). There are many advantages of single-molecule assays over traditional ensemble measurements. Besides providing the ensemble-averaged values, rare events can be detected that would be masked in ensemble measurements, and subpopulations and intermediates are observable. Furthermore, kinetic information can be determined directly in equilibrium without the need for synchronization, as can be achieved in bulk, for instance, by stopped-flow mixing. Also the widths of the experimentally determined distributions provide information

regarding the extent of heterogeneity in the biomolecular system investigated.

Particularly in protein folding, transient intermediate molecular states are hidden in bulk measurements because the proteins are not synchronized. In chaperone-assisted protein folding, the system may be even more heterogeneous. A protein may not only be in different folded states but may also be interacting with a chaperone that is in different states. Different single molecule techniques vary in their ability to detect intermediates and can provide complementary information as illustrated in Figure 2c,d. Two folding processes are displayed schematically: one in which folding commences by local interactions and another in which a long-range interaction is first established and followed by local ones. Detectability of the folding intermediates depends on the single molecule approaches used, the design of the experiment, and the protein

under study. For example, when the folded part of the protein increases progressively in size through local interactions, the end-to-end distance of the molecule reduces along the folding pathway and can be monitored by optical tweezers (Figure 2d). For the protein that folds via a long-range interaction followed by short-range ones (Figure 2c), folding steps that involve short-range interactions are not resolvable by optical tweezers. On the other hand, single-pair Förster resonance energy transfer (spFRET) based assays with dye molecules bound to the appropriate locations within the protein structure can resolve the hidden conformations.

When investigating dynamics, bulk studies are only useful when the system can be perturbed from equilibrium as has been done for time-resolved X-ray crystallography,<sup>42</sup> two-dimensional infrared spectroscopy,<sup>43</sup> and stopped-flow spectroscopy.<sup>44</sup> In such cases, transient molecular events can be followed at fast time scales:<sup>42,43</sup> stopped-flow with milliseconds dead times; continuous flow with microsecond dead times; and quenched-flow (separation of reaction and detection), pressure, or temperature jump methods (rapid unfolding) and methods with caged substrates on the nanosecond time scale. In the case of single-molecule measurements, kinetics and dynamic information as well as information on hidden intermediates are immediately available from equilibrium measurements.<sup>45</sup> In Figure 3a, three scenarios are compared: in the first scenario (type I) a single protein with a two-state folding pathway is studied: the observer follows the state of the protein as a function of time. This allows one to measure the dwell time between the two states and compile the transition probability histogram, which is indicated in Figure 3a. A chaperone could reduce the transition energy barrier between the two states and simply increase the folding rate. Alternatively, a chaperone may change the folding pathway of the protein, e.g., by stabilizing a transition intermediate. Two experimental single-molecule schemes are presented in Figure 3a to study such changes. In one assay (type II), the intermediate is not detected directly, while in another one (type III) the intermediate and the individual reaction rates are independently measured. The shape of the compiled dwell time histogram in the type II experiment indicates the existence of the intermediates, and even in special cases, the reaction rates and the number of intermediates can be inferred.<sup>45,46</sup> However, when multiple on-pathway intermediates with varying transition energy barriers are visited and when off-pathway intermediates are populated, direct detection of the intermediates (as in type III) are required to measure the kinetics and the nature of the intermediates.

Single-molecule assays further allow one to simplify complex reactions by controlling the number of possible intermolecular interactions (Figure 3b). In complex molecular systems with multiple components and several competing reaction pathways, it is often impossible to disentangle the roles of individual parts, as intermolecular interactions can lead to emergent properties. For instance, in bulk protein refolding assays, the measured emergence of protein function can be suppressed by folding delays of individual proteins as well as by interactions between multiple off- and on-pathway intermediates leading to aggregation. Moreover, interactions between the reaction intermediates can introduce nonlinearity into the reaction kinetics. The single molecule approach can be informative by simplifying the system. Figure 3b shows how one can control the number of possible interactions by designing appropriate single molecule assays. The FK binding protein (FKBP) and

the maltose binding protein (MBP) are proteins that self-interact with opposite impact on their folding yields. FKBP catalyzes its own folding, while MBP is prone to aggregation and is client to several chaperones.<sup>47</sup> Experiments can be designed to study the folding of a single FKBP or MBP in the absence of any interacting partner. Interacting partners can then be added one by one and the influence of each partner investigated.

In the scenarios presented in Figure 3, we have a single client protein, which acts as the reporter molecule, while the chaperones (and cochaperones) are many and not detectable directly. Similar experiments can be designed in which one chaperone molecule is directly detected and surrounded by many nondetectable interacting client proteins.

### 3. SINGLE-MOLECULE EXPERIMENTS ON CHAPERONES AND ASSISTED PROTEIN FOLDING

Protein folding at the single molecule level has predominantly been studied using fluorescence methods (section 3.1) and force spectroscopy (section 3.2). Fluorescence methods can be readily applied to proteins that contain naturally fluorescent compounds or can be labeled with synthetic fluorophores. By introducing fluorescent labels at specific positions in the protein or chaperone, it is possible to use Förster resonance energy transfer (FRET) to investigate the structure, conformation, interactions, and dynamics of the substrate–chaperone system. FRET is the radiationless transfer of energy through dipole–dipole interactions from a donor molecule to an acceptor molecule.<sup>48</sup> The transfer efficiency depends on the local environment, the spectral overlap of the donor fluorescence emission spectrum, and the absorption spectrum of the acceptor, the relative orientation of the donor and acceptor dipole moments, and the spatial distance ( $\sim r^{-6}$ ) between the donor and the acceptor molecules.<sup>49</sup> When an acceptor is in close proximity to the donor molecule, the emission intensity, fluorescence lifetime, and polarization of the emission (with respect to excitation) of the donor changes, and enhanced fluorescence from the acceptor is detected.<sup>50</sup> FRET can be used to probe the proximity of two regions in a single molecule or a pair of interacting molecules on the scale of 2–10 nm, as we will describe in section 3.4.

In force spectroscopy, the system under study can be perturbed mechanically, for example, by pulling the ends of linear molecules. Optical tweezers (OT) and atomic force microscope (AFM) have been used to perturb a folded protein and force it to fully unfolded or to partially folded states. By monitoring the extension length as a function of force, intermediate conformations in the unfolding and folding pathways can be visualized. In addition, after mechanical unfolding of the protein, the refolding pathway can be investigated by relaxing the applied force and monitoring the extent of refolding as a function of refolding time. As application of force alters the energy landscape of folding, an external force can be applied to make the energies of folded and unfolded states similar, and spontaneous fluctuations between these conformations can be monitored as a function of time. Forces and distances can be monitored in real time with piconewton and nanometer resolution.

In single-molecule studies of assisted protein folding, the molecular system under investigation is complex. It involves substrates, chaperones and often other additional cochaperones. Diverse protein and chaperone states are visited during this process, and limited types of probes exist to identify them.

The events in assisted protein folding happen on a wide range of time scales from microseconds to minutes. One has to keep in mind that the assay itself may alter the folding pathway. For example, in pulling assays, one typically holds the protein termini during the folding process, which may interfere with the folding. Fortunately, protein termini are typically surface exposed, and configurations in which the termini are embedded within the core typically are misfolds.<sup>51</sup> In fluorescence assays, the fluorophores can also interfere with the folding process or function due to physical interactions. Thus, it is thus possible that the landscapes measured by these assays are not exactly the same and may differ to some extent from the landscape of the unlabeled protein free in solution. In the following, we will discuss how the fluorescence and force spectroscopic methods have been applied to investigate chaperone-assisted folding processes.

### 3.1. Single-Molecule Techniques—Fluorescence Methods

**3.1.1. Single-Pair Förster Resonance Energy Transfer (FRET).** FRET is based on the energy transfer between two fluorophores when they are in close proximity. This is the most prevalent fluorescence-based single-molecule method currently in use. As the transfer rate is proportional to the sixth power of the distance between the donor and acceptor molecules, the method is very sensitive to distances and dynamics on the molecular scale. Two basic spFRET approaches are used: either single-molecule experiments are performed in solution, where single molecules freely diffuses through the observation volume of a confocal microscope, or the biomolecules of interest are immobilized on surfaces and investigated using TIRF microscopy. Solution-based measurements have the advantage that the molecules do not need to be immobilized, which could potentially impact the dynamics of the molecules. The photons emitted from individual molecules are binned together and analyzed. The use of elaborate excitation and detection schemes such as alternating laser excitation,<sup>64</sup> pulsed interleaved excitation,<sup>65</sup> or multiparameter fluorescence detection<sup>66</sup> can be used to obtain information over the stoichiometry, fluorescence lifetime,<sup>67</sup> or anisotropy<sup>68</sup> of the measured biomolecules. Single-molecule lifetime-based FRET measurements are independent of fluorescence intensity, and thus, the effect of intensity noise can be eliminated.<sup>69</sup> Transitions from the unfolded to the folded state may be followed by diluting chemically denatured proteins into nondenaturing buffers using stop-flow techniques and microfluidics.<sup>70</sup> The disadvantage of solution-based measurements is that the experiments are limited to the diffusion time of the molecules through the focus of the microscope, usually on the order of a few milliseconds, only offering a snapshot of the conformation of the protein. spFRET dynamics can be measured on longer time scales by immobilizing the proteins of interest near a coverslip using various methods.<sup>71</sup> TIRF microscopy is typically used in this case to minimize the axial size of the excitation volume and thereby minimize background. Information regarding the number of conformations, which transitions are possible between the different conformations, and their dynamics can be extracted from the data using, for example, hidden Markov modeling.<sup>72</sup>

**3.1.2. Fluorescence Correlation Spectroscopy (FCS).** FCS analyzes the information available in the fluctuations in fluorescence intensity.<sup>73</sup> These experiments are typically performed in solution with freely diffusing molecules and measured using a confocal microscope. Fluctuations in

fluorescence intensity can arise from such phenomena as variations in the number of molecules within the observation volume, molecular rotation, quenching of the fluorophores, excitation into and return from the triplet state, and changes in FRET efficiency. From the calculated autocorrelation function, the concentration of labeled molecules, their translational and/or rotational diffusion coefficient, information on the internal dynamics of molecules,<sup>74</sup> and the number of conformational states and their relative populations can be extracted.<sup>75</sup> As the size and shape of a protein changes as it folds and unfolds, it is possible to investigate folding via changes in the diffusion coefficient.<sup>76</sup>

**3.1.3. Photoinduced Electron Transfer (PET).** PET is based on quenching of a fluorophore by electron transfer from a close by quencher.<sup>77</sup> Typically, tryptophan is used as a quencher in proteins and guanine in nucleic acids. The rate of quenching depends exponentially on the distance between the fluorophore and the quencher and is an excellent probe for studying short-range interactions ( $d < 2$  nm). The technique allows for extraction of kinetics information from protein as they fold or unfold<sup>78</sup> below the range possible by FRET.<sup>78b</sup> However, direct distance information is not available.<sup>70</sup> PET as well as FRET can have been combined with FCS to extract information about dynamics of proteins on the sub-microsecond time scale.<sup>70</sup>

### 3.2. Single Molecule Techniques—Force Methods

**3.2.1. Atomic Force Microscopes (AFM).** AFM have a sharp tip mounted on a cantilever that can be used to pull on proteins that are tethered to the surface. Force probing (10 pN up to several nanonewtons<sup>91</sup>) is then achieved by measuring the deflection of the cantilever from its resting position. The amplitude and phase of oscillation and/or resonance frequency of the cantilever may be affected in response to changes in the interaction force.<sup>92</sup> The AFM is well-suited for unfolding studies: it has been used to unfold proteins<sup>93</sup> and detect transient unfolding intermediates due to the fast response provided by the stiff cantilevers. Applicability of AFM to folding studies is limited by its force resolution and drift.<sup>94</sup> A general drawback of single-molecule force methods is their invasiveness. Measurements rely on the application of a force, which affects folding. This influence may be limited by allowing folding in the absence of a force and using pulling to assess the resulting conformation of the protein. A general advantage is that force can be used to populate intermediate states that would be difficult to detect otherwise and to assess their stability, either in isolation or in complex with chaperones.

**3.2.2. Optical Tweezers.** Optical tweezers exploit the restoring force exerted by a focused laser on a dielectric particle to keep the particle near the focus of the laser.<sup>95</sup> Forces applied to tethered proteins are typically in the range of 0.5–65 pN. By measuring the force between two optical traps,<sup>96</sup> drift from the microscopy can be eliminated, leading to stable measurements, which can be further improved using correction algorithms.<sup>97</sup> Drawbacks of optical tweezers include having to link the biomolecule to beads and the need for a significant distance between beads, which is typically achieved by engineering DNA tethers to the protein termini. Recently, tethers based on covalent connections<sup>98</sup> and Avidin family proteins<sup>99</sup> have been developed that provide connections resistant to force, laser heating, and oxidative damages.<sup>100</sup>

**3.2.3. Solid-State Nanopores.** Devices with solid-state nanopores can employ electrical forces<sup>101</sup> or forces generated

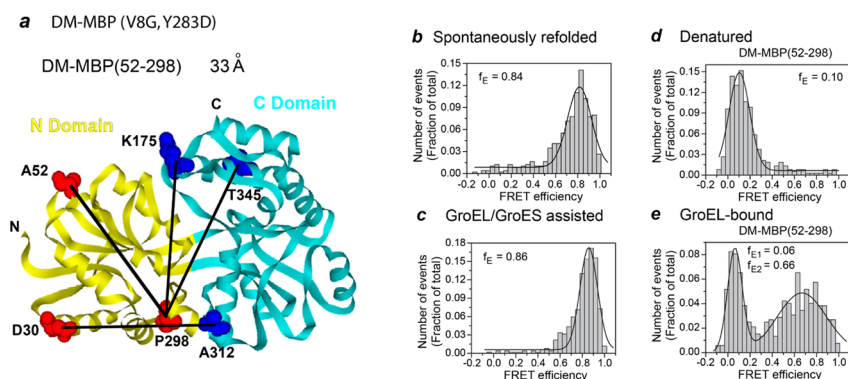


**Figure 4.** Single-pair FRET Analysis of DM-MBP in spontaneous and chaperonin-assisted folding. (a) A ribbon diagram of the structure of MBP (PDB code 1OMP) with the N-terminal domain shown in yellow and the C-terminal domain in blue. The positions of engineered cysteines are indicated in red (N domain) and blue (C domain). (b–e) Single-pair FRET measurements of double-labeled DM-MBP (52–298). GdnHCl-denatured double-labeled DM-MBP (3 nM) was diluted 50-fold (60 pM final concentration) either into buffer alone (b) or into buffer containing 3  $\mu$ M GroEL/6  $\mu$ M GroES/2 mM ATP and allowed to refold (c), diluted in 3 M GdnHCl (d), or with 3  $\mu$ M GroEL alone (e). Peak values of a Gaussian fit to the FRET efficiency distributions ( $f_E$ ) are indicated. Representative histograms of at least two independent measurements are shown. (Figure is adapted from ref 79 with permission.)

by integrated optical traps<sup>102</sup> or AFMs<sup>103</sup> to translocate proteins through a pore in a solid film (e.g., SiN<sub>x</sub>) or a biological pore.<sup>104</sup> The technique allows for forced unfolding of proteins and can distinguish between folded and unfolded states.<sup>101,105</sup> Recently it has become possible to monitor a protein during unfolding by measuring the residence time and current blockade.<sup>106</sup>

### 3.3. Initial Single-Molecule Experiments on Chaperones and Folding

Interestingly, chaperones were one of the first systems investigated using single molecule methodologies. The AFM images of the GroEL/GroES cochaperon system were published by Mou et al in 1996.<sup>52</sup> They could directly observe the 7-fold symmetry of the chaperonin system, and complexes that were bound with GroES could be distinguished from those that did not have a GroES bound. The direct interaction of GroEL/GroES with substrates was investigated using total-internal reflection fluorescence (TIRF) microscopy in 1999 by the group of Goto.<sup>53</sup> GroEL was labeled with TMR, and substrates (bovine  $\beta$ -lactoglobulin and bovine rhodanese) were labeled with Cy5. Dual-color TIRF microscopy showed colocalization of the substrates with GroEL.

The first reported single-molecule unfolding–refolding measurements were carried out using optical tweezers and AFM on the muscle protein titin in 1997.<sup>54</sup> Shortly thereafter, in 2000, single-molecule FRET was used to study the folding and unfolding pathway of proteins.<sup>55</sup> These early studies offered proof-of-principles for single molecule investigation of protein folding. The results were in agreement with previous ensemble measurements,<sup>56</sup> while adding novel insights into the stepwise unfolding and refolding dynamics.

Since these initial studies, single molecule experiments on isolated proteins have led to important advances, including the identification of a set of folding intermediates for calmodulin<sup>57</sup> (by OT), an estimation of the transition path time for protein folding<sup>58</sup> (by FRET), kinetic measurements of cotranslational folding<sup>59</sup> (by OT), identification of the role of topology in folding cooperativity<sup>60</sup> (by OT), and discovery of a misfolding/off-pathway intermediate<sup>20b,61</sup> (by OT) and metastable intermediates<sup>20b,62</sup> (by FRET) allowing for construction of energy landscape for complex proteins. Single-molecule

methods have also been used to investigate the conformational dynamics of intrinsically disordered proteins (by FRET).<sup>56,63</sup>

### 3.4. Fluorescence Experiments

Single-molecule FRET has been used to follow chaperone-assisted folding and unfolding of proteins in real time with high temporal (millisecond) resolution at the single molecule level. Sharma et al.<sup>79</sup> engineered several double-cysteine mutants for donor–acceptor labeling within a slow folding mutant of the maltose binding protein (DM-MBP). DM-MBP is an ideal system for investigating how GroEL accelerates protein folding, as the substrate will fold spontaneously over several minutes but folds up to 13 times faster in the presence of the chaperonin. The authors ensured that the labeling did not affect the folding rate of the protein. Stopped-flow ensemble FRET measurements showed that, in the absence of the barrel-shaped chaperonin GroEL, the protein collapses to a compact state within milliseconds. In the presence of GroEL, after the initial collapse, the protein expands rapidly with a  $t_{1/2}$  on the order of 100 ms. SpFRET was used to study the structural heterogeneity of client proteins upon binding to GroEL binding (Figure 4). In the absence of chaperone, the protein adopts a uniformly compact conformation within the first 200 s of spontaneous refolding.

Binding to GroEL induces fast unfolding and the emergence of a heterogeneous conformational distribution of the client protein with molecules populating both compact and locally expanded states. Steady-state anisotropy and FRET measurements performed at different locations along the polypeptide chain of DM-MBP showed that ATP binding to GroEL induced release of parts of the substrate, while other regions experienced an additional stretching of the substrate before it was released and encapsulated in the folding cavity.

In a further study, Chakraborty et al.<sup>20b</sup> used spFRET data to support the thesis that GroEL/GroES can rescue a protein from a kinetically trapped state. This is consistent with the idea that GroEL can unfold a misfolded protein and give it a new opportunity to refold properly. Hofmann et al.<sup>80</sup> reported spFRET results that show differential effects of the chaperonin system on folding rates of different domains of the substrate protein rhodanese. The results showed that confinement in the chaperonin decelerates the folding of the C-terminal domain of the substrate protein rhodanese while the folding rate of the N-

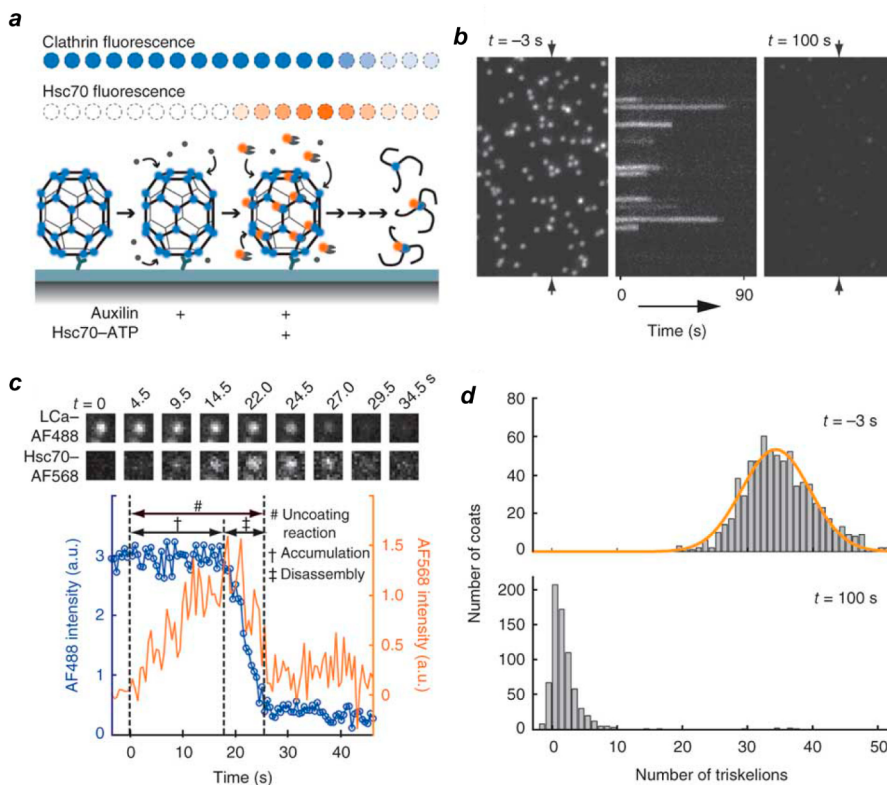


**Figure 5.** (a) A schematic representation of the single-particle uncoating assay for clathrin-coated pits. The fluorescence intensities from labeled clathrin and Hsc70 were monitored using TIRF microscopy for clathrin/AP-2 coats captured on the surface of a PEG-modified glass coverslip. (b) Representative time traces of a single-particle uncoating assay. The left and right panels show the first and last frames of the fluorescence channel used to monitor the signal from coats tagged with clathrin LCa–AF488, respectively, and the middle panel shows a kymograph generated from the vertical axis indicated by the arrows in the left panel showing the unsynchronized disappearance of clathrin fluorescence. Hsc70–ATP ( $1.2 \mu\text{M}$ ) arrived in the flow chamber at  $t = 0$ . (c) The uncoating profile from a single coat. The selected snapshots from the time series (top panels) show the fluorescence from clathrin and Hsc70 in the selected coat at various time points during the uncoating reaction carried out with  $0.9 \mu\text{M}$  Hsc70. The snapshots are background-corrected averages of three successive frames. The plot shows intensity traces of the clathrin (blue) and Hsc70 (orange) signals. The  $t = 0$  time point is the moment at which a rapid increase in Hsc70 background signal is recorded; this event corresponds to the arrival of Hsc70 within the evanescent field at the coverslip. (d) Histogram of the number of trimers (triskelions) per coat at the beginning (top) and the end (bottom) of the single-particle uncoating assay carried out with  $1.2 \mu\text{M}$  Hsc70. The number of trimers in intact coats follows a normal distribution with a mean of 34 triskelions per coat (top panel). In most cases, only one or two trimers remained at the site of a coat at the end of the reaction (bottom panel). Objects with overlapping point-spread functions were excluded from this analysis (au, arbitrary units). (Figure is adapted from ref 87 with permission.)

terminal domain was unaffected. The results show that the influence of the chaperonin depends on the substrate. This approach opens the door to establishing the mechanism of how GroEL affects the conformation of its client proteins and helps them fold.<sup>81</sup>

A key aspect in resolving the mechanism of GroEL-assisted protein folding is the conformational dynamics of the chaperonin itself. Interconversion of GroEL between its two allosteric states (T and R) has been investigated using the PET-FCS technique at the single molecule level. This study<sup>74</sup> investigated a double mutant (F44W, K327C) of the single-ring version of the GroEL at various levels of ATP concentrations. The T state exhibits a low affinity for ATP, while the R state has high affinity for ATP.<sup>82</sup> In the T conformation, the incorporated tryptophan quenches the fluorescence label and becomes visible as an additional relaxation in the autocorrelation function on the microsecond time scale. The FCS experiments showed that, even at ATP saturation,  $\sim 50\%$  of the molecules adopt the T state at the steady state, indicating constant out-of-equilibrium cycling between the T and R forms.<sup>74</sup> This is in contrast with thermodynamic predictions,

which suggests that only the R form should be populated at high [ATP]. The dominant formation of R at high [ATP] is, however, in agreement with the existing model for the chaperone cycle.<sup>74</sup>

To understand how chaperones modulate protein folding, it is important to know the number of chaperones bound to a single client protein. Fluorescence cross-correlation spectroscopy (FCCS) has been used to assess the stoichiometry of chaperone–protein complexes.<sup>83</sup> Sharma et al.<sup>79</sup> used pulsed interleaved excitation (PIE)<sup>65</sup> in conjunction with FCCS to verify that only one substrate (MBP) is bound to GroEL at a time.

To further probe the interplay between GroEL and its clients, TIRF microscopy based single-molecule experiments of GFP refolding in the cavity of GroEL/GroES were performed by the group of Funatsu.<sup>84</sup> While the fluorescence recovery behaved as a single exponential process in the absence of chaperone, in the presence of GroEL–GroES–ATP, the fluorescence recovery showed a delay of nearly 3 s. The lag time indicated a conformational transition in the apical domain, which, in turn, is required for unbinding of GFP from the

domain and encapsulation in the cavity. This transition was followed by a second transition with slightly slower kinetics ( $\tau \sim 5$  s) before the substrate was released at the end of the chaperone cycle. Hence, the authors proposed a so-called “two timer pathway” for GroEL/GroES assisted protein folding.<sup>84</sup>

SpFRET studies have also addressed the structural heterogeneity of mitochondrial Ssc1, a chaperone from the HSP70/DnaK family, by measuring distributions of FRET efficiencies.<sup>85</sup> Surprisingly, while the ATP state showed structural uniformity, the ADP state was found to be heterogeneous in conformation. Similar results were obtained in spFRET measurements for the endoplasmic reticulum Hsp70 homologue<sup>27a</sup> and in bulk electron paramagnetic resonance measurements for *E. coli* Hsp70.<sup>28</sup> By encapsulating Ssc1 in 200 nm large vesicles and immobilizing the vesicles to a quartz prism, surface-based spFRET could be performed to follow the dynamics of Ssc1 in real time over minutes.<sup>27b</sup> These experiments verified that the heterogeneity detected previously in the ADP state is due to dynamic fluctuations between a nucleotide-free and ADP-bound conformation. Upon identification of different conformations via their FRET efficiency, Ssc1 was encapsulated in vesicles with substrate and ATP, and the dynamics of the conformational cycle was followed. The authors could show that the chaperone was in a nucleotide-bound conformation immediately before substrate binding and that, upon dissociation of the substrate, Ssc1 returned to a nucleotide-bound conformation without going through the nucleotide-free state.

In another study, the group of Hugel used surface-based spFRET with Hsp90 dimers caged in lipid vesicles to study the conformational fluctuations and dimerization of the chaperone at its C- and N-terminal interfaces.<sup>37,86</sup> Surprisingly, they found that the fluctuations between the open and closed state of the N-terminus of Hsp90 occurred on a much faster time scale than ATP hydrolysis and showed that ATP hydrolysis and the conformational cycle are not tightly coupled. Opening and closing of the C-terminal dimer were also observed with fast kinetics. Dimerization of the C- and N-terminal domains was found to be anticorrelated and binding of nucleotides destabilized the closed conformation of the C-terminal domains. These studies offer an exciting first view into the complex conformation dynamics of Hsp70 and Hsp90 chaperones and their coupling with the ATP hydrolysis cycle. It would be intriguing to observe how these dynamics are affected by interacting clients, and vice versa, how client conformations are affected by these interactions.

The chaperone-assisted disassembly of clathrin-coated vesicles was studied using single-particle fluorescence imaging combined with microfluidics and TIRF illumination (Figure 5). Böcking et al.<sup>87</sup> studied how Hsc70, a member of Hsp70 family, catalyzes a large-scale disassembly reaction in real time. Single clathrin coats were fluorescently labeled and immobilized on a coverslip within a micro fluidic channel. Fluorescently labeled chaperone was flowed through the sample cell and the binding of the Hsc70 to the clathrin-coated pits and the final uncoating was followed via the fluorescence intensity using TIRF microscopy. The authors found that once the Hsc70 reached a critical concentration of one Hsc70 molecule per two binding sites, a rapid cooperative uncoating of the vesicle follows. These results are consistent with bulk studies indicating that Hsp70 can act as an “unfoldase”.<sup>88</sup>

Elegant single-molecule experiments were performed in the group of Moerner using an anti-Brownian electrokinetic

(ABEL) trap. The ABEL trap generates electrophoretic and electroosmotic forces by applying a voltage to electronic leads positioned near the focus of a confocal microscope with single-molecule sensitivity to keep fluorescently labeled molecules in the focal volume.<sup>89</sup> By canceling the Brownian motion of the molecule, the molecule can be effectively immobilized while being still free in solution. Hence, it combines the advantages of solution measurements with that of immobilization. Jiang and co-workers used the ABEL trap to immobilize single TRiC molecules and counted the number of fluorescently labeled ADP and ADP-ALFX molecules attached to the chaperonin.<sup>90</sup> By determining the stoichiometry of ADP-Cy3 attached to TRiC complex as a function of time, it was found that the number of complexes containing fluorescently labeled ADP decreased with time while the fluorescently labeled complexes usually still had eight ADP molecules bound. This suggests a high cooperativity within TRiC that leads to the rapid release of all eight ADP molecules

### 3.5. Force Spectroscopy and Pulling Experiments

In mechanical manipulation approaches (see section 3.2), proteins are held via their termini between a flat surface and a cantilever (in the case of AFM) or between two micrometer size beads (in the case of optical tweezers). By applying mechanical force to the molecular ends, the proteins are stretched and forced to unfold. The end-to-end distance of the protein can be monitored during the experiment. The methods can also be used to study protein folding, by relaxing the unfolded protein and then monitoring both the force and the effective protein end-to-end distance by consecutive pulls with different waiting times.

Bechtluft et al.<sup>47b</sup> used optical tweezers to demonstrate how SecB, the ATP-independent *E. coli* chaperone involved in protein translocation across the plasma membrane, modulates the folding pathway of MBP (Figure 6). MBP unfolding was found to occur in two steps: first, a C-terminal part ( $\sim 28$  nm) was unfolded resulting in an MBP core intermediate. The core intermediate then unfolded in one step. During MBP folding, the extended peptide is compacted to a molten globule state followed by folding of the MBP core. The effect of SecB was found to be specific: tertiary contacts were effectively blocked in the transition to the core state while the transition from the core to the native state was unaffected by SecB (Figure 6e,f). Suppression of tertiary contacts had been also observed for GroEL using NMR spectroscopic techniques and computational modeling.<sup>107</sup> By analyzing a tandem 4MBP construct that during refolding is highly prone to misfolding (Figure 3b), SecB was found to prevent the stable aggregation interactions between MBP molecules and thus to significantly alter the folding pathway of MBP. These findings illustrate the benefit of single-molecule methods: the ability to probe how individual folding transitions within the larger folding pathway are affected by chaperones. Hence, this approach opens the door to studying whether and how chaperones such as Hsp70, Hsp90, and trigger factor influence the conformational search of folding protein chains.

In two other studies, Aubin-Tam et al. and Maillard et al. demonstrated how ClpXP and ClpX unfold individual protein domains in a highly cooperative manner prior to their degradation.<sup>108</sup> Their finding supports a power-stroke model of denaturation, in which enzyme-mediated unfolding of stable protein domains involves concurrence of mechanical pulling of the template through the enzyme pore and a transient

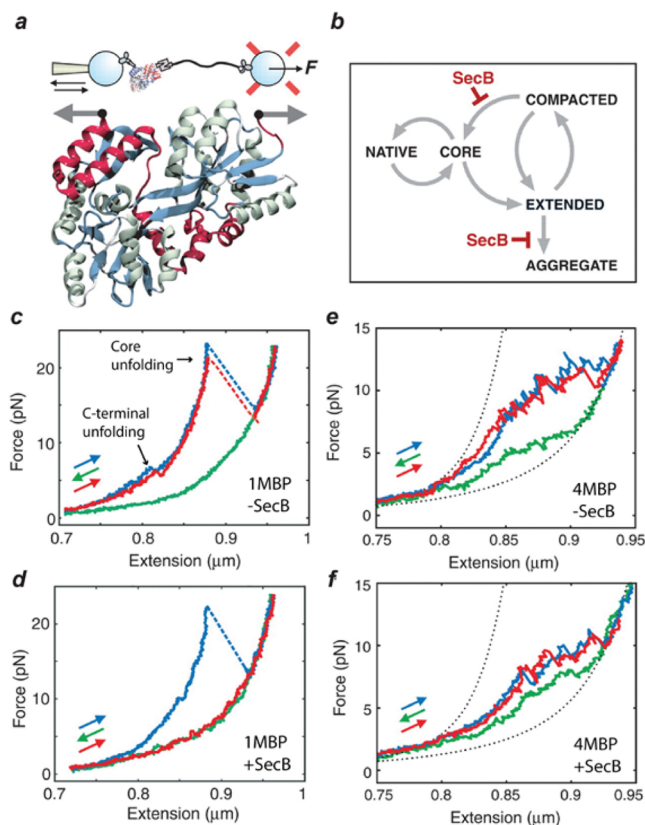


**Figure 6.** Force-induced unfolding of MBP. (a) A schematic of the experimental setup is shown. MBP is tethered between the two beads: One is held on a position-controlled micropipet, the other is held by an optical trap that detects the applied force. At the C-terminus, MBP is attached via an antibody–myc-tag connection, whereas at the N-terminus it is attached via streptavidin–biotin linkages to a DNA tether, which in turn is attached to the bead surface via an antibody–digoxigenin connection. (b) A model showing the force-induced MBP folding and unfolding transitions observed in the experiments and their dependence on SecB. (c) Force–extension curves were measured in the absence of SecB showing unfolding at high force (blue), refolding at low forces (green), and again unfolding at high force (red). (d) Force–extension curves measured in the presence of SecB ( $0.1 \mu\text{M}$ ). The second stretching curve (red) lacks the typical unfolding features, showing that stable tertiary interactions are absent. (e) Force–extension curves of the C-terminal regions of 4MBP in the absence of SecB. The construct was first stretched, resulting in the predicted gradual unfolding of the external  $\alpha$ -helices (red helices in panel a), and then relaxed before the core structures could unfold. During relaxation, the near-equilibrium refolding of the same  $\alpha$ -helices was observed directly as a shortening of the tether. The dotted lines indicate the wormlike chain model (WLC) behavior: The first denotes the DNA alone, whereas, in the second, a  $4 \times 91$  residue-compliant polypeptide was added, representing the unfolded external  $\alpha$ -helices. (f) Force–extension curves of the C-terminal regions of 4MBP in presence of SecB ( $0.1 \mu\text{M}$ ). The SecB interactions do not alter this refolding transition. (Figure is adapted from ref 47b with permission.)

stochastic reduction in protein stability. This interplay between the client and chaperone dynamics is visible in particular at the single-molecule level and central to understanding the mechanisms that chaperones employ. It will be of interest to explore whether similar peptide-liberation mechanisms are also used in other ring-like chaperone systems, such as those involved in disaggregation.

AFM has been applied to image chaperones to gain structural insight or to assay their binding and localization: Structural

analyses of GroEL, GroES, and oligomeric GroES have been performed using liquid AFM.<sup>52,109</sup> It has also been used to confirm the presence of Hsp60 on the membrane of stressed cells at a high lateral resolution.<sup>110</sup> In another study, Zhu et al.<sup>111</sup> found that the small heat shock protein  $\alpha\text{B}$ -crystallin interacts and protects cardiac titin from damage. This is achieved by lowering the persistence length of the titin N2B-U<sub>s</sub> element and by reducing the unfolding rate of the Ig domain flanking the N2B-U<sub>s</sub>.

AFM experiments have been conducted to probe binding of chaperones to client proteins as well as stabilization of the clients. Here, one of the interaction partners is attached on the surface, while the other is connected to the AFM tip. An AFM study showed that interaction forces between substrates (destabilized mutant of citrate synthase and beta-lactamase) and GroEL decrease in the presence of ATP (but not ATP- $\gamma$ -S) and that the force is smaller for natively proteins than for the fully denatured ones.<sup>109b</sup> Such AFM methods may be expanded to probe the nature of client–chaperone complexes by monitoring in detail how the client is removed from the interacting GroEL chaperone. AFM has also been used to analyze interactions of  $\alpha$ -synuclein with microbial esterases. The interaction of  $\alpha$ -synuclein with esterase appears to be highly specific and can protect the native conformation of esterase.<sup>112</sup>

### 3.6. In Silico Single-Molecule Methods

Although molecular simulations have yielded important insights into mechanistic aspects of folding of individual proteins in isolation, they have rarely been used to study chaperone-assisted protein folding problem,<sup>113</sup> either co- or post-translationally. Such simulations have not been tractable due to the large system size and the enormous computational cost involved. Some in silico studies exist on the structure and dynamics of chaperones without client and on chaperone-assisted protein folding. Unbiased all-atom molecular dynamics simulations of the GroEL subunit protein have been performed with and without ATP. The study revealed inter-ring cooperativity and nucleotide-dependent conformational transitions in GroEL.<sup>114</sup> Fan et al.<sup>115</sup> studied the facilitation of folding of a partially folded protein using a coarse grained model of GroEL/GroES. The chaperone was simulated as a hydrophobic box that allows repeated binding and release of substrate. Folding then proceeds under spatial confinement. The study led to the conclusion that folding of encapsulated proteins is facilitated under spatial confinement.

The role of confinement in folding has been investigated in a number of simulation and theoretical studies. Of particular interest has been the direct role (in contrast with the passive antiaggregation role<sup>116</sup>) of confinement in protein folding and unfolding,<sup>117</sup> folding pathway,<sup>118</sup> and protein stability.<sup>119</sup> The formation of various motifs such as the  $\beta$ -hairpin<sup>120</sup> and the  $\alpha/\beta$ -sandwich fold<sup>117b</sup> and even small proteins with different  $\alpha/\beta$ -content<sup>121</sup> have been simulated under confinement with spherical, cylindrical, or cubic geometries. Jewett et al. considered patchy surfaces with attractive hydrophobic and repulsive hydrophobic interactions.<sup>122</sup> Others considered purely repulsive walls.<sup>117b,121,123</sup> One can also generate cavities by using many repulsive spheres, which simulates the effects of crowding.<sup>124</sup> In general, the picture emerging from these studies is that confinement results in an increased thermodynamic stability and more compact unfolded conformation.

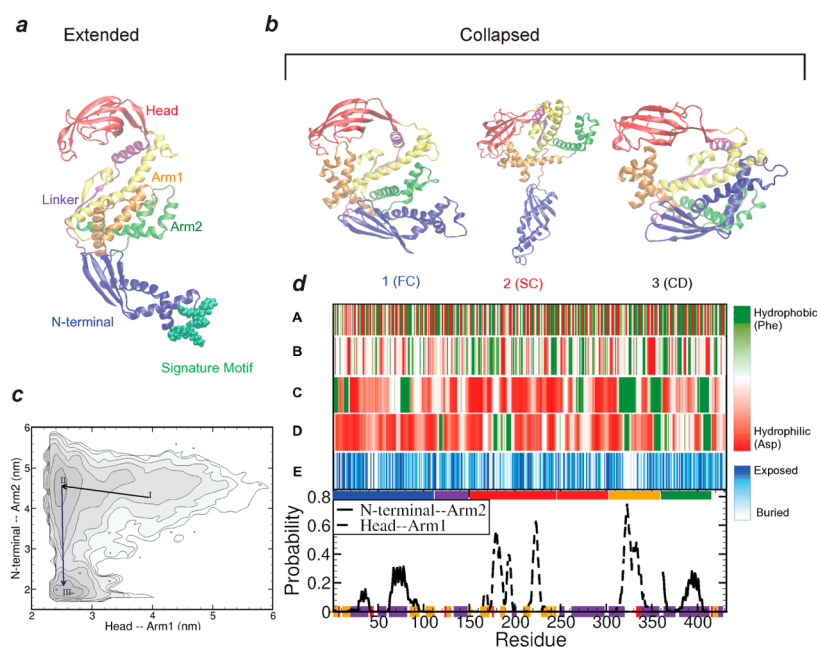


**Figure 7.** Simulations of trigger factor conformational dynamics: (a) crystal structure of trigger factor (TF) monomer (PDB code 1W26), with its N-terminal domain (blue), PPIase domain (red, also called “head”), and C-terminal domain consisting of two armlike extensions (Arm1, orange; Arm2, green). The signature motif acts as the binding site for the ribosome. (b) Three collapsed structures observed during the simulation time, showing contacts between the arms and head or N-terminus. (c) Free energy plot for distance between Head and Arm1 vs N-terminal and Arm2 shows three regions corresponding to initial extended structure (I), semicollapsed (II), and the completely collapsed conformation (III). The deepest well corresponds to the completely collapsed conformation. Contour lines represent a free energy difference of 1 *kT*. (d) Hydrophobicity of TF is displayed as a colored barcode: (A) standard hydrophobicity of TF per residue, (B) standard hydrophobicity of TF residues, (C) in the extended state and (D) in the collapsed state (FC). (E) Barcode representing the extent of buried (white) and exposed (blue) residues upon collapse. (F) These plots are overlaid on the probability graph of formation of contact pairs in NtA2 and HA1 collapses. (Figure is adapted from ref 127 with permission.)

The average structure of DnaK–DnaJ complex was obtained by MD simulation.<sup>125</sup> Liwo et al simulated the full transition of an Hsp70 from the SBD-closed to the SBD-open conformation by conducting canonical and multiplexed replica exchange simulations of the conformational dynamics of Hsp70s using a coarse-grained molecular dynamics approach with the united-residue (UNRES) force field.<sup>126</sup> The results confirmed the experimentally observed influence of ATP-binding on the transition of Hsp70s from the SBD-closed to the SBD-open form.<sup>7</sup>

The nucleotide dependence of the dynamics and structural heterogeneity of Hsp90 have been studied recently using novel simulation methods. In one study, comparisons were performed of the dynamics of Hsp90 from different sources. Morra et al. considered the fluctuations of the distances of all pairs of amino acids (based on several hundred nanosecond atomistic MD simulations) and thereby found the regions subject to the largest deformation of their structural neighborhood upon exchange of the nucleotide from ATP to ADP.<sup>128</sup> To gain insight into motions at the scale of domains, a minimalistic quasirigid domain description was used. The results pointed toward two functional sites important in nucleotide-mediated structural changes, one being at the interface of the middle domain and N-terminal domain and a second one within the middle domain. In another study, using molecular dynamics simulations combined with principal component analysis and the energy landscape model, a network of conserved regions was identified with a possible functional role in coordinating functional dynamics, principal collective motions, and allosteric signaling of Hsp90 and its homologues.<sup>129</sup>

Atomistic molecular dynamic simulation<sup>127</sup> on single trigger factor have indicated that the solution structure of trigger factor collapses into various compact structures (Figure 7a–c) that are remarkably different from the crystal structure (and its structure on the ribosome). To understand the functioning of the chaperones and their interactions with clients, the surface properties of the chaperones are central. Surface hydrophobicity is commonly estimated typically by considering the hydrophobicity of the individual residues.<sup>130</sup> However, as the hydrophobic effect is a collective phenomenon, the surface properties may not be properly determined from the individual residues. Recently, a method was proposed on the basis of neutral Lennard-Jones methane-like particles as hydrophobic probes to characterize the hydrophobicity of protein surfaces more accurately.<sup>131</sup> This method has been recently applied to characterize the surface of trigger factor<sup>127</sup> (Figure 7d).

With new developments in coarse graining protocols and efficient atomistic modeling approaches, we expect that silico studies of chaperones and chaperone-assisted protein folding, combined with single-molecule experiments, to become a very powerful tool for unraveling the mechanism of chaperone-assisted protein folding.

#### 4. CONCLUSION

Understanding how protein chains fold into their functional state has been referred to as one of the grand challenges of modern science.<sup>14c</sup> Understanding the decisive events of this elementary process would open the door to predicting complex protein structures and functions from DNA sequence data and to engineering non-natural proteins with novel functions.

Moreover, mechanistic insights into the folding errors and protein aggregation that underlie many medical and aging conditions are essential for eventually developing rational approaches for therapeutic intervention.

Studying chaperone-assisted protein folding poses considerable challenges, as the functions of chaperones are diverse and a large number of cochaperones participate, while at the same time the effect of the chaperone may be substrate dependent. Although single-molecule studies have already contributed to a deeper understanding of assisted protein folding, we have only begun to scratch the surface. Important general remaining issues include the following: providing insight into the structure and dynamics of the intermediate states in the folding pathways of complex proteins; understanding how the different chaperone systems act differently on folding pathways; probing the direct interaction between folding intermediates and chaperones; and investigating protein folding mechanisms in more complex environments, e.g., in the presence of a network of chaperones and cochaperones, with the ultimate aim of performing such experiments in living cells. These types of studies may provide insights into the consequences of a failure of the proteostasis system caused by imbalance or even absence of sufficient chaperone capacity, e.g., the development of protein misfolding diseases<sup>132</sup> and other biologically relevant processes as well as details regarding the pathways protein chaperone-assisted protein folding. Issues specific to different chaperones are discussed in section 1.1.

Studying the structure of folding intermediate states using traditional methods of structural biology is often not feasible, because of the dynamic nature of both the client and chaperone and the low occupancy of transient intermediate states. Single-molecule methods provide a way to start addressing this issue. Force-based methods have been used to directly probe intermediate folded states and may thus be used to explore whether chaperones promote their occurrence. Because the measurements occur in real time, one could attempt to determine whether chaperones alter the sequence of states that are visited as a protein folds. Whether chaperones indeed interact with intermediate folds may also be studied directly, for instance, by quantifying the forces required to unfold them or by measuring their lifetime in the absence or presence of applied force. Misfolding interactions within proteins have been detected by optical tweezers,<sup>57,61b</sup> and hence, one can investigate whether chaperones are able to specifically suppress these transitions. While aggregation necessarily involves multiple proteins, one can mimic aggregation in constructs where protein monomers are arranged head to tail.<sup>47b</sup> Such constructs allow one to address how chaperones are able to fight aggregation while still allowing folding. spFRET on multiple labeling sites allows one to determine the position of flexible regions in proteins or even entire structures.<sup>133</sup> As spFRET can identify subpopulations, the structures of the different subpopulations can be determined independently, even for dynamics complexes. Hence, one may employ this method to follow how a chaperone affects the folding dynamics of specific regions along the protein chain.

Single-molecule methods allow one not only to study the conformation and dynamics of chaperones and their influence on the conformation of substrates but also to investigate the protein-folding landscape.<sup>57,98</sup> Similar methods could be used to explore how folding landscapes are altered by chaperones. By binding and unbinding substrate proteins, chaperones could protect protein chain regions from unwanted interactions

within and between proteins and, hence, improve the folding yield. By interacting with hydrophobic side chains, chaperones will increase the entropy since water will be released. Local unfolding could increase conformational entropy of the chain but at the same time decrease the overall entropy due to ordered binding of water to hydrophobic side chains. In the folding landscape, this would correspond to increasing the barrier to the aggregated state. It has often been speculated that chaperones have more elaborate mechanisms with a more direct role in protein folding. Chaperones such as GroEL, which provide a folding cavity for their substrates, may aid protein folding by confinement, thereby lowering the entropy and consequently raising the energy of the unfolded state and lowering the barrier to the native state. One may also speculate that chaperone interactions lower the barrier to the native state by stabilizing the folding transition state in a manner that resembles a classical catalyst. Alternatively, chaperones may produce new intermediates and, hence, steer folding pathways along them toward the native fold. These types of questions are now directly addressable using single-molecule techniques.

As chaperone-assisted folding pathways involve a number of players and interactions, one of the next steps for single-molecule experiments on chaperones is to increase the complexity of the systems. This can be done in a multitude of ways. For example, in spFRET and PET experiments, one can incorporate more components into lipid or polymeric vesicles.<sup>71e,134</sup> Microfluidic devices can be used to allow rapid mixing and dilution for investigating protein unfolding and refolding. In this way, different components (e.g., substrates, chaperones and cochaperons, and nucleotides) can be added at controlled time points and known concentrations. To allow a more detailed study of the interactions of multiple components, multicolor experiments will become useful such as three- and four-color FRET.<sup>135</sup> The consequence of increasing the number of fluorescent labels goes well beyond the addition of another channel of information but allows new types of questions to be investigated regarding the coordinated interaction and dynamics of biomolecules. For example, the conformation of a protein can be monitored (e.g., with spFRET) in the presence or absence of a binding partner (labeled in a third color), or the order in which domains fold in a multidomain protein could be determined using multicolor FRET.

The ultimate single molecule assay on chaperone-assisted protein folding would be to follow protein folding inside the highly crowded living cell.<sup>136</sup> Recently, it has already become possible to measure the 3D structure of proteins within living cells using high-resolution heteronuclear multidimensional NMR spectra.<sup>137</sup> Many steps toward single-molecule folding experiments in live cells have already been taken, including the first live-cell folding experiments on the ensemble level<sup>138</sup> and single-molecules measurements in living cells<sup>139</sup> and bacteria.<sup>140</sup> Single-molecule experiments in live cells can also be complemented with experiments in isolated organelles or in cellular extracts, which are easier to perform while near-native conditions are maintained and also direct manipulation of the molecules under investigation is allowed.

In summary, single-molecule methods provide an exciting new tool to address many of the long-standing questions in chaperone-assisted protein folding. A better understanding the dynamic interplay between chaperone and client will provide a new perspective to the chaperone field and has the potential to fundamentally alter the protein-folding problem.

## AUTHOR INFORMATION

### Corresponding Authors

\*Telephone: +31-20-7547303. Fax: +31-20-6684106. E-mail: mashaghi@amolf.nl.

\*Telephone: +31-20-7547100. Fax: +31-20-6684106. E-mail: tans@amolf.nl.

### Author Contributions

The manuscript was written through contributions of all authors. All authors have given approval to the final version of the manuscript.

### Funding

This work was supported by the research program of the Foundation for Fundamental Research on Matter (FOM), which is part of The Netherlands Organisation for Scientific Research (NWO). D.C.L. gratefully acknowledges funding through the Deutsche Forschungsgemeinschaft [SFB 1035 and the Nanosystems Initiative Munich (NIM)] and the Ludwig-Maximilians-University Munich (LMUInnovativ BioImaging Network).

### Notes

The authors declare no competing financial interest.

### Biographies



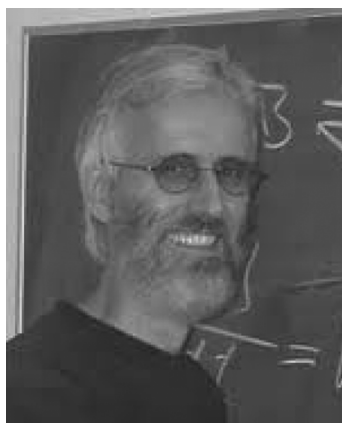
Alireza Mashaghi received his M.D. degree with honors from Tehran University of Medical Sciences in 2003 with a thesis on immunogenetics. While studying at the medical school he developed interest in pursuing a parallel track science career and became the first Iranian student with a dual education. He studied chemistry (B.Sc.), theoretical physics (M.Sc.), and biological physics (M.Sc.) at the University of Tehran and Sharif University of Technology. His research was focused on the statistical physics of networks. He then moved to Europe and worked on the development of fluorescence correlation spectroscopy to study asymmetric cell division at Max Planck Institute (MPI) for Molecular Cell Biology and Genetics and on high-resolution NMR spectroscopy at MPI for Biophysical Chemistry. Further, he did postdiploma work in materials science at ETH Zürich, where he designed and conducted various projects on nanotechnology, surface science, and optical/plasmonic sensing. He then worked at the FOM institute AMOLF studying single-molecule protein folding, molecular topology, and ultrafast dynamics of biomolecules and received his Ph.D. with highest distinction in physics from Delft University of Technology. He is an editorial board member of *Scientific Reports*.



Günter Kramer received his Diploma (Biology) and Ph.D. degree from the University of Konstanz, Germany. After his Ph.D., he did first postdoctoral work at the University of Freiburg focusing on the mechanistic analysis of chaperones interacting with ribosomes and nascent polypeptides. In 2003 he became a Alexander von Humboldt Research Fellow at the Whitehead Institute for Biomedical Research and Massachusetts Institute of Technology working on the impact of molecular chaperones in evolution. In 2005, he joined the Center for Molecular Biology (ZMBH) at the University of Freiburg, Germany, where he currently works as a project leader. His work focuses on mechanisms coordinating protein synthesis with downstream maturation processes of the nascent polypeptide.



Don C. Lamb is a full professor at the Department of Physical Chemistry, Ludwig-Maximilians-University, Munich, Germany. He received his Bachelor's degree in Physics and Mathematics from Illinois Wesleyan University and his Masters degree in Physics from the University of Illinois at Urbana–Champaign. He obtained his Ph.D. in Physics in 1993 at the University of Illinois at Urbana–Champaign with a thesis on molecular physiology of myoglobin. After his Ph.D. studies, he became a research fellow at Massachusetts General Hospital and Harvard Medical School, where his research was focused on laser interactions with tissues. In 1995 he moved to Technische Universität München as an Alexander von Humboldt Research Fellow to work on photoinduced relaxations in myoglobin. In 2003, he became a group leader at the Department of Physical Chemistry, Ludwig-Maximilians-University, where he is currently a full professor. His research interest is in utilizing fluorescence and single molecule methods to investigate the dynamics and functions of biomolecules. He acted as a Guest Editor of *ChemPhysChem* for a special issue on single molecules in 2012.



Matthias P. Mayer received his Diploma degree (Biology) and a Ph.D. from the University of Freiburg. After a postdoctoral stay at the University of Utah (1990–92) and the University of Geneva (1992–1997) he moved back to the University of Freiburg as a senior research scientist. In 2002, he joined the Zentrum für Molekulare Biologie, University of Heidelberg, where he heads an independent research group. His research focus is on the molecular mechanism of Hsp70 and Hsp90 chaperone systems. He is the winner of 2002 Ernst Schering Research Foundation Habilitation Prize of the Society for Biochemistry and Molecular Biology (GBM).



Sander J. Tans received M.Sc. degrees in Applied Physics from Université Jussieu (1991) and Delft University of Technology (1993). He obtained his Ph.D. with highest distinctions from Delft University of Technology, where he conducted research on the electronic properties of single carbon nanotubes. In 1999, he joined the University of California at Berkeley as a postdoctoral fellow to measure the activity of single DNA packaging motors using optical tweezers. In 2001, he became a group leader at FOM institute AMOLF. Since 2009 he holds a part-time appointment as a full professor at the Kavli Institute of NanoScience, Delft University of Technology. His main research areas include single-molecule biophysics, systems biology, and evolutionary biology. He won a number of awards, including a VIDJ grant (2005) and a VICI grant (2012) from NWO, The Netherlands.

## ACKNOWLEDGMENTS

The authors are grateful to Dr. Stephen Helms, Dr. Francois Anquez, and Dr. Katja Taute for comments on an earlier manuscript and valuable discussions.

## REFERENCES

(1) (a) Ellis, R. J.; Minton, A. P. *Biol. Chem.* **2006**, *387*, 485. (b) White, D. A.; Buell, A. K.; Knowles, T. P. J.; Welland, M. E.; Dobson, C. M. *J. Am. Chem. Soc.* **2010**, *132*, 5170.

- (2) (a) Creighton, T. E. *Proc. Natl. Acad. Sci. U. S. A.* **1988**, *85*, 5082. (b) Kubelka, J.; Hofrichter, J.; Eaton, W. A. *Curr. Opin. Struct. Biol.* **2004**, *14*, 76.
- (3) Ellis, R. J. *Trends Biochem. Sci.* **2001**, *26*, 597.
- (4) Kuhn, T.; Ihalainen, T. O.; Hyvaluoma, J.; Dross, N.; Willman, S. F.; Langowski, J.; Vihinen-Ranta, M.; Timonen, J. *Plos One* **2011**, *6*, e22962.
- (5) Krishna, M. M. G.; Lin, Y.; Englander, S. W. *J. Mol. Biol.* **2004**, *343*, 1095.
- (6) Bertelsen, E. B.; Chang, L.; Gestwicki, J. E.; Zuiderweg, E. R. P. *Proc. Natl. Acad. Sci. U. S. A.* **2009**, *106*, 8471.
- (7) Kityk, R.; Kopp, J.; Sinning, I.; Mayer, M. P. *Mol. Cell* **2012**, *48*, 863.
- (8) Ranson, N. A.; Clare, D. K.; Farr, G. W.; Houldershaw, D.; Horwich, A. L.; Saibil, H. R. *Nat. Struct. Mol. Biol.* **2006**, *13*, 147.
- (9) Shiau, A. K.; Harris, S. F.; Southworth, D. R.; Agard, D. A. *Cell* **2006**, *127*, 329.
- (10) Ali, M. M. U.; Roe, S. M.; Vaughan, C. K.; Meyer, P.; Panaretou, B.; Piper, P. W.; Prodromou, C.; Pearl, L. H. *Nature* **2006**, *440*, 1013.
- (11) Langer, T.; Lu, C.; Echols, H.; Flanagan, J.; Hayer, M. K.; Hartl, F. U. *Nature* **1992**, *356*, 683.
- (12) (a) Shorter, J. *PLoS One* **2011**, *6*, e26319. (b) Tyedmers, J.; Mogk, A.; Bukau, B. *Nat. Rev. Mol. Cell Biol.* **2010**, *11*, 777. (c) Rampelt, H.; Kirstein-Miles, J.; Nillegoda, N. B.; Chi, K.; Scholz, S. R.; Morimoto, R. I.; Bukau, B. *EMBO J.* **2012**, *31*, 4221.
- (13) Wegele, H.; Muller, L.; Buchner, J. *Rev. Physiol. Biochem. Pharmacol.* **2004**, *151*, 1.
- (14) (a) Hartl, F. U.; Bracher, A.; Hayer-Hartl, M. *Nature* **2011**, *475*, 324. (b) Bukau, B.; Weissman, J.; Horwich, A. *Cell* **2006**, *125*, 443. (c) Walter, S.; Buchner, J. *Angew. Chem. Int. Ed.* **2002**, *41*, 1098. (d) Mayer, M. P. *Mol. Cell* **2010**, *39*, 321. (e) Dobson, C. M. *Nature* **2003**, *426*, 884. (f) Dill, K. A.; MacCallum, J. L. *Science* **2012**, *338*, 1042.
- (15) (a) Xu, Z. H.; Horwich, A. L.; Sigler, P. B. *Nature* **1997**, *388*, 741. (b) Zhang, J. J.; Baker, M. L.; Schroder, G. F.; Douglas, N. R.; Reissmann, S.; Jakana, J.; Dougherty, M.; Fu, C. J.; Levitt, M.; Ludtke, S. J.; Frydman, J.; Chiu, W. *Nature* **2010**, *463*, 379.
- (16) Chaudhuri, T. K.; Farr, G. W.; Fenton, W. A.; Rospert, S.; Horwich, A. L. *Cell* **2001**, *107*, 235.
- (17) (a) Kerner, M. J.; Naylor, D. J.; Ishihama, Y.; Maier, T.; Chang, H. C.; Stines, A. P.; Georgopoulos, C.; Frishman, D.; Hayer-Hartl, M.; Mann, M.; Hartl, F. U. *Cell* **2005**, *122*, 209. (b) Fujiwara, K.; Ishihama, Y.; Nakahigashi, K.; Soga, T.; Taguchi, H. *EMBO J.* **2010**, *29*, 1552.
- (18) Hyeon, C.; Lorimer, G. H.; Thirumalai, D. *Proc. Natl. Acad. Sci. U. S. A.* **2006**, *103*, 18939.
- (19) Horwich, A. L.; Fenton, W. A. *Q. Rev. Biophys.* **2009**, *42*, 83.
- (20) (a) Tang, Y. C.; Chang, H. C.; Roeben, A.; Wischniewski, D.; Wischniewski, N.; Kerner, M. J.; Hartl, F. U.; Hayer-Hartl, M. *Cell* **2006**, *125*, 903. (b) Chakraborty, K.; Chatila, M.; Sinha, J.; Shi, Q. Y.; Poschner, B. C.; Sikor, M.; Jiang, G. X.; Lamb, D. C.; Hartl, F. U.; Hayer-Hartl, M. *Cell* **2010**, *142*, 112.
- (21) Brinker, A.; Pfeifer, G.; Kerner, M. J.; Naylor, D. J.; Hartl, F. U.; Hayer-Hartl, M. *Cell* **2001**, *107*, 223.
- (22) Horowitz, A. *NATO Sci. Peace Security Ser. A: Chem. Biol.* **2012**, *79*.
- (23) Mayer, M. P.; Bukau, B. *Cell. Mol. Life Sci.* **2005**, *62*, 670.
- (24) Willmund, F.; del Alamo, M.; Pechmann, S.; Chen, T. T.; Albanese, V.; Dammer, E. B.; Peng, J. M.; Frydman, J. *Cell* **2013**, *152*, 196.
- (25) Mayer, M. P.; Schroder, H.; Rudiger, S.; Paal, K.; Laufen, T.; Bukau, B. *Nat. Struct. Biol.* **2000**, *7*, 586.
- (26) Zhu, X. T.; Zhao, X.; Burkholder, W. F.; Gragerov, A.; Ogata, C. M.; Gottesman, M. E.; Hendrickson, W. A. *Science* **1996**, *272*, 1606.
- (27) (a) Marcinowski, M.; Holler, M.; Feige, M. J.; Baerend, D.; Lamb, D. C.; Buchner, J. *Nat. Struct. Mol. Biol.* **2011**, *18*, 150. (b) Sikor, M.; M., K.; von Voithenberg, L. V.; Mokranjac, D.; Lamb, D. C. *EMBO J.* **2013**, *32*, 1639.
- (28) Schlecht, R.; Erbse, A. H.; Bukau, B.; Mayer, M. P. *Nat. Struct. Mol. Biol.* **2011**, *18*, 345.

- (29) Szabo, A.; Langer, T.; Schroder, H.; Flanagan, J.; Bukau, B.; Hartl, F. U. *Proc. Natl. Acad. Sci. U. S. A.* **1994**, *91*, 10345.
- (30) (a) Diamant, S.; Ben-Zvi, A. P.; Bukau, B.; Goloubinoff, P. J. *Biol. Chem.* **2000**, *275*, 21107. (b) Schroder, H.; Langer, T.; Hartl, F. U.; Bukau, B. *EMBO J.* **1993**, *12*, 4137.
- (31) Sharma, S. K.; De Los Rios, P.; Christen, P.; Lustig, A.; Goloubinoff, P. *Nat. Chem. Biol.* **2010**, *6*, 914.
- (32) Rosenzweig, R.; Moradi, S.; Zarrine-Afsar, A.; Glover, J. R.; Kay, L. E. *Science* **2013**, *339*, 1080.
- (33) Rudiger, S.; Germeroth, L.; SchneiderMergener, J.; Bukau, B. *EMBO J.* **1997**, *16*, 1501.
- (34) Rodriguez, F.; Arsene-Ploetze, F.; Rist, W.; Rudiger, S.; Schneider-Mergener, J.; Mayer, M. P.; Bukau, B. *Mol. Cell* **2008**, *32*, 347.
- (35) Stankiewicz, M.; Nikolay, R.; Rybin, V.; Mayer, M. P. *FEBS J.* **2010**, *277*, 3353.
- (36) Malyshev, I. *Springer Briefs Biochem. Mol. Biol.* **2013**, *6*, 15.
- (37) Ratzke, C.; Mickler, M.; Hellenkamp, B.; Buchner, J.; Hugel, T. *Ptoc. Natl. Acad. Sci. U. S. A.* **2010**, *107*, 16101.
- (38) Li, J.; Soroka, J.; Buchner, J. *Biochim. Biophys. Acta* **2012**, *1823*, 624.
- (39) Liu, S.; Li, P.; Dybkov, O.; Nottrott, S.; Hartmuth, K.; Luhrmann, R.; Carlomagno, T.; Wahl, M. C. *Science* **2007**, *316*, 115.
- (40) Lakowicz, J. R. *Principles of Fluorescence Spectroscopy*, 3rd ed.; Springer: New York, 2006.
- (41) Feng, D.; Jin, G. *Introduction to Condensed Matter Physics*; World Scientific: Hackensack, NJ, 2005.
- (42) Schotte, F.; Lim, M. H.; Jackson, T. A.; Smirnov, A. V.; Soman, J.; Olson, J. S.; Phillips, G. N.; Wulff, M.; Anfirud, P. A. *Science* **2003**, *300*, 1944.
- (43) Kolano, C.; Helbing, J.; Kozinski, M.; Sander, W.; Hamm, P. *Nature* **2006**, *444*, 469.
- (44) (a) Frieden, C.; Hoeltzli, S. D.; Ropson, I. J. *Protein Sci.* **1993**, *2*, 2007. (b) Fabian, H.; Naumann, D. *Methods* **2004**, *34*, 28.
- (45) Floyd, D. L.; Ragains, J. R.; Skehel, J. J.; Harrison, S. C.; van Oijen, A. M. *Proc. Natl. Acad. Sci. U. S. A.* **2008**, *105*, 15382.
- (46) Floyd, D. L.; Harrison, S. C.; van Oijen, A. M. *Biophys. J.* **2010**, *99*, 360.
- (47) (a) Scholz, C.; Zarnt, T.; Kern, G.; Lang, K.; Burtscher, H.; Fischer, G.; Schmid, F. X. *J. Biol. Chem.* **1996**, *271*, 12703. (b) Bechtluft, P.; van Leeuwen, R. G.; Tyreman, M.; Tomkiewicz, D.; Nouwen, N.; Tepper, H. L.; Driessen, A. J.; Tans, S. J. *Science* **2007**, *318*, 1458.
- (48) (a) Förster, T. *Naturwissenschaften* **1946**, *6*, 166. (b) Förster, T. *Ann. Phys. (Leipzig)* **1948**, *2*, 55.
- (49) (a) Clegg, R. M. *Methods Enzymol.* **1992**, *211*, 353. (b) Roy, R.; Hohng, S.; Ha, T. *Nat. Methods* **2008**, *5*, 507.
- (50) Schuler, B.; Eaton, W. A. *Curr. Opin. Struct. Biol.* **2008**, *18*, 16.
- (51) Jacob, E.; Unger, R. *Bioinformatics* **2007**, *23*, E225.
- (52) (a) Mou, J. X.; Czajkowsky, D. M.; Sheng, S. J.; Ho, R. Y.; Shao, Z. F. *FEBS Lett.* **1996**, *381*, 161. (b) Mou, J. X.; Sheng, S. T.; Ho, R. Y.; Shao, Z. F. *Biophys. J.* **1996**, *71*, 2213.
- (53) Yamasaki, R.; Hoshino, M.; Wazawa, T.; Ishii, Y.; Yanagida, T.; Kawata, Y.; Higurashi, T.; Sakai, K.; Nagai, J.; Goto, Y. *J. Mol. Biol.* **1999**, *292*, 965.
- (54) (a) Kellermayer, M. S. Z.; Smith, S. B.; Granzier, H. L.; Bustamante, C. *Science* **1997**, *276*, 1112. (b) Tskhovrebova, L.; Trinick, J.; Sleep, J. A.; Simmons, R. M. *Nature* **1997**, *387*, 308. (c) Rief, M.; Gautel, M.; Oesterhelt, F.; Fernandez, J. M.; Gaub, H. E. *Science* **1997**, *276*, 1109.
- (55) (a) Deniz, A. A.; Laurence, T. A.; Beligere, G. S.; Dahan, M.; Martin, A. B.; Chemla, D. S.; Dawson, P. E.; Schultz, P. G.; Weiss, S. *Proc. Natl. Acad. Sci. U. S. A.* **2000**, *97*, 5179. (b) Talaga, D. S.; Lau, W. L.; Roder, H.; Tang, J. Y.; Jia, Y. W.; DeGrado, W. F.; Hochstrasser, R. M. *Proc. Natl. Acad. Sci. U. S. A.* **2000**, *97*, 13021.
- (56) Ferreon, A. C. M.; Deniz, A. A. *Biochim. Biophys. Acta, Proteomics* **2011**, *1814*, 1021.
- (57) Stigler, J.; Ziegler, F.; Gieseke, A.; Gebhardt, J. C.; Rief, M. *Science* **2011**, *334*, 512.
- (58) Chung, H. S.; McHale, K.; Louis, J. M.; Eaton, W. A. *Science* **2012**, *335*, 981.
- (59) Kaiser, C. M.; Goldman, D. H.; Chodera, J. D.; Tinoco, I., Jr.; Bustamante, C. *Science* **2011**, *334*, 1723.
- (60) Shank, E. A.; Cecconi, C.; Dill, J. W.; Marqusee, S.; Bustamante, C. *Nature* **2010**, *465*, 637.
- (61) (a) Xi, Z.; Gao, Y.; Sirinakis, G.; Guo, H.; Zhang, Y. *Proc. Natl. Acad. Sci. U. S. A.* **2012**, *109*, 5711. (b) Yu, H.; Liu, X.; Neupane, K.; Gupta, A. N.; Brigley, A. M.; Solanki, A.; Sosova, I.; Woodside, M. T. *Proc. Natl. Acad. Sci. U. S. A.* **2012**, *109*, 5283.
- (62) Pirchi, M.; Ziv, G.; Riven, I.; Cohen, S. S.; Zohar, N.; Barak, Y.; Haran, G. *Nat. Commun.* **2011**, *2*, 493.
- (63) Choi, U. B.; McCann, J. J.; Weninger, K. R.; Bowen, M. E. *Structure* **2011**, *19*, 566.
- (64) (a) Kapanidis, A. N.; Lee, N. K.; Laurence, T. A.; Doose, S.; Margeat, E.; Weiss, S. *Proc. Natl. Acad. Sci. U. S. A.* **2004**, *101*, 8936. (b) Lee, N. K.; Kapanidis, A. N.; Wang, Y.; Michalet, X.; Mukhopadhyay, J.; Ebright, R. H.; Weiss, S. *Biophys. J.* **2005**, *88*, 2939.
- (65) Müller, B. K.; Zaychikov, E.; Brauchle, C.; Lamb, D. C. *Biophys. J.* **2005**, *89*, 3508.
- (66) (a) Kudryavtsev, V.; Sikor, M.; Kalinin, S.; Mokranjac, D.; Seidel, C. A.; Lamb, D. C. *ChemPhysChem* **2012**, *13*, 1060. (b) Kühnemuth, R.; Seidel, C. A. M. *Single Mol.* **2001**, *2*, 251.
- (67) Eggeling, C.; Fries, J. R.; Brand, L.; Gunther, R.; Seidel, C. A. *Proc. Natl. Acad. Sci. U. S. A.* **1998**, *95*, 1556.
- (68) Sisamakias, E.; Valeri, A.; Kalinin, S.; Rothwell, P. J.; Seidel, C. A. M. *Method Enzymol.* **2010**, *475*, 455.
- (69) He, Y.; Lu, M.; Lu, H. P. *Phys. Chem. Chem. Phys.* **2013**, *15*, 770.
- (70) Schuler, B.; Hofmann, H. *Curr. Opin. Struct. Biol.* **2013**, *23*, 36.
- (71) (a) Jia, Y. W.; Talaga, D. S.; Lau, W. L.; Lu, H. S. M.; DeGrado, W. F.; Hochstrasser, R. M. *Chem. Phys.* **1999**, *247*, 69. (b) Kuzmenkina, E. V.; Heyes, C. D.; Nienhaus, G. U. *Proc. Natl. Acad. Sci. U. S. A.* **2005**, *102*, 15471. (c) Pal, P.; Lesoine, J. F.; Lieb, M. A.; Novotny, L.; Knauf, P. A. *Biophys. J.* **2005**, *89*, L11. (d) Rhoades, E.; Cohen, M.; Schuler, B.; Haran, G. *J. Am. Chem. Soc.* **2004**, *126*, 14686. (e) Okumus, B.; Wilson, T. J.; Lilley, D. M.; Ha, T. *Biophys. J.* **2004**, *87*, 2798.
- (72) McKinney, S. A.; Joo, C.; Ha, T. *Biophys. J.* **2006**, *91*, 1941.
- (73) (a) Elson, E. L.; Magde, D. *Biopolymers* **1974**, *13*, 1. (b) Magde, D.; Elson, E. L.; Webb, W. W. *Phys. Rev. Lett.* **1972**, *29*, 705. (c) Magde, D.; Elson, E. L.; Webb, W. W. *Biopolymers* **1974**, *13*, 29. (d) *Methods in Enzymology. Fluorescence Fluctuation Spectroscopy (FFS)*; Tetin, S. Y., Ed.; Academic Press: New York, 2013; Vol. 519, Part B. (e) *Methods in Enzymology. Fluorescence Fluctuation Spectroscopy (FFS)*; Tetin, S. Y., Ed.; Academic Press: New York, 2013; Vol. 518, Part A.
- (74) Frank, G. A.; Gomanovsky, M.; Davidi, A.; Ziv, G.; Horovitz, A.; Haran, G. *Proc. Natl. Acad. Sci. U. S. A.* **2010**, *107*, 6270.
- (75) Frank, G. A.; Horovitz, A.; Haran, G. *Methods Mol. Biol.* **2012**, *796*, 205.
- (76) Bismuto, E.; Maggio, E. D.; Pleus, S.; Sikor, M.; Röcker, C.; Nienhaus, G. U.; Lamb, D. C. *Proteins: Struct., Funct. Bioinf.* **2009**, *74*, 273.
- (77) Doose, S.; Neuweiler, H.; Sauer, M. *ChemPhysChem* **2009**, *10*, 1389.
- (78) (a) Neuweiler, H.; Banachewicz, W.; Fersht, A. R. *Proc. Natl. Acad. Sci. U. S. A.* **2010**, *107*, 22106. (b) Neuweiler, H.; Johnson, C. M.; Fersht, A. R. *Proc. Natl. Acad. Sci. U. S. A.* **2009**, *106*, 18569.
- (79) Sharma, S.; Chakraborty, K.; Mueller, B. K.; Astola, N.; Tang, Y. C.; Lamb, D. C.; Hayer-Hartl, M.; Hartl, F. U. *Cell* **2008**, *133*, 142.
- (80) Hofmann, H.; Hillger, F.; Pfeil, S. H.; Hoffmann, A.; Streich, D.; Haenni, D.; Nettels, D.; Lipman, E. A.; Schuler, B. *Proc. Natl. Acad. Sci. U. S. A.* **2010**, *107*, 11793.
- (81) Jewett, A. I.; Shea, J. E. *Cell. Mol. Life Sci.* **2010**, *67*, 255.
- (82) Grason, J. P.; Gresham, J. S.; Widjaja, L.; Wehri, S. C.; Lorimer, G. H. *Proc. Natl. Acad. Sci. U. S. A.* **2008**, *105*, 17334.
- (83) Schwill, P.; MeyerAlmes, F. J.; Rigler, R. *Biophys. J.* **1997**, *72*, 1878.
- (84) Ueno, T.; Taguchi, H.; Tadakuma, H.; Yoshida, M.; Funatsu, T. *Mol. Cell* **2004**, *14*, 423.

- (85) Mapa, K.; Sikor, M.; Kudryavtsev, V.; Waegemann, K.; Kalinin, S.; Seidel, C. A. M.; Neupert, W.; Lamb, D. C.; Mokranjac, D. *Mol. Cell* **2010**, *38*, 89.
- (86) (a) Mickler, M.; Hessling, M.; Ratzke, C.; Buchner, J.; Hugel, T. *Nat. Struct. Mol. Biol.* **2009**, *16*, 281. (b) Ratzke, C.; Berkemeier, F.; Hugel, T. *Proc. Natl. Acad. Sci. U. S. A.* **2012**, *109*, 161.
- (87) Böcking, T.; Aguet, F.; Harrison, S. C.; Kirchhausen, T. *Nat. Struct. Mol. Biol.* **2011**, *18*, 295.
- (88) Sharma, S. K.; De los Rios, P.; Christen, P.; Lustig, A.; Goloubinoff, P. *Nat. Chem. Biol.* **2010**, *6*, 914.
- (89) (a) Cohen, A. E.; Moerner, W. E. *Appl. Phys. Lett.* **2005**, *86*, 093109. (b) Fields, A. P.; Cohen, A. E. *Methods Enzymol.* **2010**, *475*, 149.
- (90) Jiang, Y.; Douglas, N. R.; Conley, N. R.; Miller, E. J.; Frydman, J.; Moerner, W. E. *Proc. Natl. Acad. Sci. U. S. A.* **2011**, *108*, 16962.
- (91) Neuman, K. C.; Nagy, A. *Nat. Methods* **2008**, *5*, 491.
- (92) (a) Okajima, T.; Arakawa, H.; Alam, M. T.; Sekiguchi, H.; Ikai, A. *Biophys. Chem.* **2004**, *107*, 51. (b) Janovjak, H.; Muller, D. J.; Humphris, A. D. L. *Biophys. J.* **2005**, *88*, 1423. (c) Forbes, J. G.; Wang, K. J. *Vac. Sci. Technol. A* **2004**, *22*, 1439. (d) Higgins, M. J.; Sader, J. E.; Jarvis, S. P. *Biophys. J.* **2006**, *90*, 640.
- (93) Garcia, R.; Herruzo, E. T. *Nat. Nanotechnol.* **2012**, *7*, 217.
- (94) Zoldak, G.; Rief, M. *Curr. Opin. Struct. Biol.* **2013**, *23*, 48.
- (95) Ashkin, A.; Dziedzic, J. M.; Bjorkholm, J. E.; Chu, S. *Opt. Lett.* **1986**, *11*, 288.
- (96) (a) Moffitt, J. R.; Chemla, Y. R.; Izhaky, D.; Bustamante, C. *Proc. Natl. Acad. Sci. U. S. A.* **2006**, *103*, 9006. (b) Abbondanzieri, E. A.; Greenleaf, W. J.; Shaevitz, J. W.; Landick, R.; Block, S. M. *Nature* **2005**, *438*, 460.
- (97) Mashaghi, A.; Vach, P. J.; Tans, S. J. *Rev. Sci. Instrum.* **2011**, *82*, 115103.
- (98) Cecconi, C.; Shank, E. A.; Bustamante, C.; Marqusee, S. *Science* **2005**, *309*, 2057.
- (99) Moayed, F.; Mashaghi, A.; Tans, S. J. *PLoS One* **2013**, *8*, e54440.
- (100) Landry, M. P.; McCall, P. M.; Qi, Z.; Chemla, Y. R. *Biophys. J.* **2009**, *97*, 2128.
- (101) Talaga, D. S.; Li, J. J. *Am. Chem. Soc.* **2009**, *131*, 9287.
- (102) Keyser, U. F.; Koeleman, B. N.; Van Dorp, S.; Krapf, D.; Smeets, R. M. M.; Lemay, S. G.; Dekker, N. H.; Dekker, C. *Nat. Phys.* **2006**, *2*, 473.
- (103) King, G. M.; Golovchenko, J. A. *Phys. Rev. Lett.* **2005**, *95*, 216103.
- (104) Rodriguez-Larrea, D.; Bayley, H. *Nat. Nanotechnol.* **2013**, *8*, 288.
- (105) Oukhaled, G.; Mathe, J.; Bianca, A. L.; Bacri, L.; Betton, J. M.; Lairaz, D.; Pelta, J.; Auvray, L. *Phys. Rev. Lett.* **2007**, *98*, 158101.
- (106) Freedman, K. J.; Haq, S. R.; Edel, J. B.; Jemth, P.; Kim, M. J. *Sci. Rep.* **2013**, *3*, 1638.
- (107) (a) Horst, R.; Bertelsen, E. B.; Fiaux, J.; Wider, G.; Horwich, A. L.; Wuthrich, K. *Proc. Natl. Acad. Sci. U. S. A.* **2005**, *102*, 12748. (b) Stan, G.; Lorimer, G. H.; Thirumalai, D.; Brooks, B. R. *Proc. Natl. Acad. Sci. U. S. A.* **2007**, *104*, 8803.
- (108) (a) Aubin-Tam, M. E.; Olivares, A. O.; Sauer, R. T.; Baker, T. A.; Lang, M. J. *Cell* **2011**, *145*, 257. (b) Maillard, R. A.; Chistol, G.; Sen, M.; Righini, M.; Tan, J. Y.; Kaiser, C. M.; Hodges, C.; Martin, A.; Bustamante, C. *Cell* **2011**, *145*, 459.
- (109) (a) Valle, F.; DeRose, J. A.; Dietler, G.; Kawe, M.; Pluckthun, A.; Semenza, G. *Ultramicroscopy* **2002**, *93*, 83. (b) Vinckier, A.; Gervasoni, P.; Zaugg, F.; Ziegler, U.; Lindner, P.; Groscurth, P.; Pluckthun, A.; Semenza, G. *Biophys. J.* **1998**, *74*, 3256.
- (110) Pfister, G.; Stroth, C. M.; Perschinka, H.; Kind, M.; Knoflach, M.; Hinterdorfer, P.; Wick, G. *J. Cell Sci.* **2005**, *118*, 1587.
- (111) Zhu, Y.; Bogomolovas, J.; Labeit, S.; Granzier, H. *J. Biol. Chem.* **2009**, *284*, 13914.
- (112) Ahn, M.; Kim, S.; Kang, M.; Ryu, Y.; Kim, T. D. *Biochem. Biophys. Res. Commun.* **2006**, *346*, 1142.
- (113) Elcock, A. H. *PLoS Comput. Biol.* **2006**, *2*, 824.
- (114) (a) Sliozberg, Y. R.; Strawhecker, K. E.; Andzelm, J. W.; Lenhart, J. L. *Soft Matter* **2011**, *7*, 7539. (b) Sliozberg, Y.; Abrams, C. F. *Biophys. J.* **2007**, *380a*. (c) Sliozberg, Y.; Abrams, C. F. *Biophys. J.* **2007**, *93*, 1906.
- (115) Fan, H.; Mark, A. E. *Protein Sci.* **2006**, *15*, 441.
- (116) Horwich, A. L.; Apetri, A. C.; Fenton, W. A. *FEBS Lett.* **2009**, *583*, 2654.
- (117) (a) Mittal, J.; Best, R. B. *Proc. Natl. Acad. Sci. U. S. A.* **2008**, *105*, 20233. (b) Baumketner, A.; Jewett, A.; Shea, J. E. *J. Mol. Biol.* **2003**, *332*, 701.
- (118) Marino, K. A.; Bolhuis, P. G. *J. Phys. Chem. B* **2012**, *116*, 11872.
- (119) (a) Zhou, H. X.; Dill, K. A. *Biochemistry* **2001**, *40*, 11289. (b) Caraglio, M.; Pelizzola, A. *Phys. Biol.* **2012**, *9*, 016006.
- (120) Klimov, D. K.; Newfield, D.; Thirumalai, D. *Proc. Natl. Acad. Sci. U. S. A.* **2002**, *99*, 8019.
- (121) Takagi, F.; Koga, N.; Takada, S. *Proc. Natl. Acad. Sci. U. S. A.* **2003**, *100*, 11367.
- (122) Jewett, A. I.; Baumketner, A.; Shea, J. E. *Proc. Natl. Acad. Sci. U. S. A.* **2004**, *101*, 13192.
- (123) (a) Rathore, N.; Knotts, T. A., IV; de Pablo, J. J. *Biophys. J.* **2006**, *90*, 1767. (b) Sirur, A.; Best, R. B. *Biophys. J.* **2013**, *104*, 1098.
- (124) Cheung, M. S.; Klimov, D.; Thirumalai, D. *Proc. Natl. Acad. Sci. U. S. A.* **2005**, *102*, 4753.
- (125) Ahmad, A.; Bhattacharya, A.; McDonald, R. A.; Cordes, M.; Ellington, B.; Bertelsen, E. B.; Zuiderweg, E. R. P. *Proc. Natl. Acad. Sci. U. S. A.* **2011**, *108*, 18966.
- (126) Golas, E.; Maisuradze, G. G.; Senet, P.; Oldziej, S.; Czaplewski, C.; Scheraga, H. A.; Liwo, A. *J. Chem. Theory Comput.* **2012**, *8*, 1750.
- (127) Singhal, K.; Vreede, J.; Mashaghi, A.; Tans, S. J.; Bolhuis, P. G. *PLoS One* **2013**, *8*, e59683.
- (128) Morra, G.; Potestio, R.; Micheletti, C.; Colombo, G. *PLoS Comput. Biol.* **2012**, *8*, e1002433.
- (129) Dixit, A.; Verkhivker, G. M. *PLoS One* **2012**, *7*, e37605.
- (130) Monera, O. D.; Sereda, T. J.; Zhou, N. E.; Kay, C. M.; Hodges, R. S. *J. Pept. Sci.* **1995**, *1*, 319.
- (131) (a) Acharya, H.; Vembanur, S.; Jamadagni, S. N.; Garde, S. *Faraday Discuss.* **2010**, *146*, 353. (b) Jamadagni, S. N.; Godawat, R.; Garde, S. *Annu. Rev. Chem. Biomol.* **2011**, *2*, 147.
- (132) McClellan, A. J.; Tam, S.; Kaganovich, D.; Frydman, J. *Nat. Cell Biol.* **2005**, *7*, 736.
- (133) (a) Kalinin, S.; Peulen, T.; Sindbert, S.; Rothwell, P. J.; Berger, S.; Restle, T.; Goody, R. S.; Gohlke, H.; Seidel, C. A. *Nat. Methods* **2012**, *9*, 1218. (b) Andrecka, J.; Treutlein, B.; Arcusa, M. A.; Muschiello, A.; Lewis, R.; Cheung, A. C.; Cramer, P.; Michaelis, J. *Nucleic Acids Res.* **2009**, *37*, 5803. (c) Muschiello, A.; Andrecka, J.; Jawhari, A.; Bruckner, F.; Cramer, P.; Michaelis, J. *Nat. Methods* **2008**, *5*, 965.
- (134) Fitter, J.; Katranidis, A.; Rosenkranz, T.; Atta, D.; Schlesinger, R.; Buldt, G. *Soft Matter* **2011**, *7*, 1254.
- (135) (a) Hohng, S.; Joo, C.; Ha, T. *Biophys. J.* **2004**, *87*, 1328. (b) Clamme, J. P.; Deniz, A. A. *ChemPhysChem* **2005**, *6*, 74. (c) Lee, J.; Lee, S.; Ragunathan, K.; Joo, C.; Ha, T.; Hohng, S. *Angew. Chem., Int. Ed.* **2010**, *49*, 9922. (d) Stein, I. H.; Steinhauer, C.; Tinnefeld, P. *J. Am. Chem. Soc.* **2011**, *133*, 4193.
- (136) Altieri, D. C. *Oncotarget* **2011**, *2*, 347.
- (137) (a) Burz, D. S.; Shekhtman, A. *Nature* **2009**, *458*, 37. (b) Sakakibara, D.; Sasaki, A.; Ikeya, T.; Hamatsu, J.; Hanashima, T.; Mishima, M.; Yoshimasu, M.; Hayashi, N.; Mikawa, T.; Walchli, M.; Smith, B. O.; Shirakawa, M.; Guntert, P.; Ito, Y. *Nature* **2009**, *458*, 102.
- (138) Guo, M.; Xu, Y.; Gruebele, M. *Proc. Natl. Acad. Sci. U. S. A.* **2012**, *109*, 17863.
- (139) Li, G. W.; Xie, X. S. *Nature* **2011**, *475*, 308.
- (140) Uphoff, S.; Reyes-Lamothe, R.; Garza de Leon, F.; Sherratt, D. J.; Kapanidis, A. N. *Proc. Natl. Acad. Sci. U. S. A.* **2013**, *110*, 8063.